Solar Energy Materials & Solar Cells 238 (2022) 111625

Contents lists available at ScienceDirect

Solar Energy Materials and Solar Cells

journal homepage: www.elsevier.com/locate/solmat

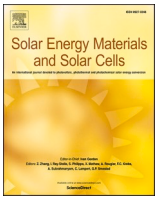

Review of the spectrally selective (CSP) absorber coatings, suitable for use in SHIP

Luka Noč, Ivan Jerman *

Department of Materials Chemistry, National Institute of Chemistry, Hajdrihova 19, 1000, Ljubljana, Slovenia

ARTICLE INFO

Keywords:
Concentrated solar power
Solar heat for industrial processes
Spectrally selective coatings
Solar absorber efficiency
Coating deposition methods
Thermal stability

ABSTRACT

A key component in the conversion process of concentrated solar power (CSP) into thermal energy is a solar absorber coating. Many experimental and simulated coatings for various substrates for CSP water/steam or molten salt absorbers have been developed. The main challenges today remain in the selection of a low-cost and effective fabrication method, appropriate for industrial production, and assessment of the degradation rate and service life of these coatings, which affect the efficiency of the plant and the LCOE. In this article, we review different types of mid- ($100 < T < 400$ °C) and high-temperature (>400 °C) absorber coatings and their fabrication methods. The emphasis is on the solar absorptance, thermal emittance and the long-term (>10 years) thermal stability of the coatings. Spectral selectivity of the coatings, which is more difficult and expensive than other means, was proven to be essential for a low-to-mid temperature range and low concentration ratios, yet for high temperatures and high concentration ratios, high solar absorptive coatings can achieve the same or even better performance than spectral selective ones. Important factors for an efficient CSP absorber are compatibility of the coating and substrate under cyclic temperature conditions and high heat transfer rate to a heat transfer medium.

1. Introduction

Within 6 h, the world's deserts receive solar energy in an amount equal to the energy produced by mankind in a year [1]. According to the International Energy Agency, 49% of world's energy demand in 2018 is in the form of heat for industrial processes and space and water heating in buildings and agriculture, while 29% of energy is used for transport and 21% is used as electricity [2].

These facts, among others, initiated the European Horizon 2020 project called Forthcoming Research and Industry for European and National Development of Solar Heat for Industrial Processes (FRIENDSHIP), with the aim to develop technology based on concentrated solar power (CSP), parabolic trough collectors (PTCs) and linear Fresnel reflectors (LFRs) in order to provide heating and cooling for industrial demands [3].

CSP is a technology that uses large sun-tracking reflective surfaces to concentrate and direct solar radiation to an absorber with a small surface area. This results in an increased concentration of solar energy at the absorber surface, where it is converted to thermal energy and is used as a heat source for electricity production or industrial process heat. The CSP plays an important role as a part of the renewable energy sources producing 6128 MW of power worldwide [4]. In the near future, the increase in 3139 MW in power production is planned with the development and construction of new CSP plants.

CSP technology is a way of concentrating sunlight divided into line-focusing (LFR, PTC) and point-focusing (ST, PD) systems with different absorber operating temperatures (T_{abs}) and concentration ratios (C) at which theoretical solar-to-thermal-to-mechanical conversion efficiency is the highest (Table 1) [5,6].

One of the strategies to raise the efficiency of a CSP plant with a solar tower absorber is to raise the operating temperature. This causes higher thermal loads on the materials, which need to have long-term stability at high temperatures and high heating and cooling rates due to day/night cycles [7].

Current operating temperatures of industrial power tower CSP plants are up to 838 K [8], but the thermal-to-mechanical (Carnot) efficiency for steam engines is temperature dependent:

$$\eta_{Carnot} = 1 - \frac{T_{low}}{T_{high}} \quad (1)$$

* Corresponding author.
E-mail address: Ivan.Jerman@ki.si (I. Jerman).

https://doi.org/10.1016/j.solmat.2022.111625
Received 22 October 2021; Received in revised form 21 December 2021; Accepted 25 January 2022
Available online 4 February 2022

Table 1
Comparison of the four CSP types by absorber temperature, concentration ratio and solar-to-mechanical energy efficiency.

CSP type	T_{abs} (°C)	C (/)	η_m
Linear Fresnel reflector (LFR)	300	~30	0.38
Parabolic trough collector (PTC)	400	~80	0.44
Solar tower (ST)	850	~500	0.67
Parabolic dish (PD)	1100	~2000	0.75

where T_{high} is operating temperature and T_{low} is ambient temperature; the increase in T_{high} up to 1383 K would increase a CSP plant's overall efficiency [9].

Another approach to raise the efficiency of CSP plants is to achieve high spectral selectivity of a solar absorber. Spectral selectivity of the absorber coating is determined by solar absorptance (α_S) and thermal emittance (ε_T), which are defined as:

$$\alpha s = \frac{\int_{0.25\ \mu m}^{2.5\ \mu m} I_s(\lambda)(1-R(\lambda))d\lambda}{\int_{0.25\ \mu m}^{2.5\ \mu m} I_s(\lambda)d\lambda} \quad (2)$$

$$\varepsilon T = \frac{\int_{1.5\ \mu m}^{16.5\ \mu m} I_b(\lambda,\ T)(1-R(\lambda))d\lambda}{\int_{1.5\ \mu m}^{16.5\ \mu m} I_b(\lambda,T)d\lambda} \quad (3)$$

where I_s (λ) is reference solar spectral irradiance AM 1.5 according to ISO standard ISO 9845-1, 1992, R (λ) is spectral reflectance and I_b (λ, T) is blackbody radiation at 80 °C [10]. Solar absorptance (α_S) and thermal emittance (ε_T) values are calculated numerically from the measured reflectance spectra at room temperature.

The efficiency of transformation of solar energy to thermal energy of the CSP absorber is described with eq. (4):

$$\eta_t = FOM = \frac{\int_{0.25\ \mu m}^{2.5\ \mu m} I_s(\lambda)(1-R(\lambda))d\lambda - \frac{1}{C}\int_{1.5\ \mu m}^{16.5\ \mu m} I_b(\lambda,\ T)(1-R(\lambda))d\lambda}{\int_{0.25\ \mu m}^{2.5\ \mu m} I_s(\lambda)d\lambda} = \alpha_S - \frac{\varepsilon_T \sigma T_{abs}^4}{CI_s} \quad (4)$$

where σ is the Stefan–Boltzmann constant, T_{abs} is the absorber's operating temperature, C is the solar concentration factor and I_S is the AM 1.5 solar spectral irradiance. The thermal conductive and convective losses of the absorber are neglected [10].

By multiplying eq. (1) by eq. (4), solar-to-mechanical conversion efficiency is obtained as a result:

$$\eta_m = \eta_{Carnot}\eta_t \quad (5)$$

Ideally, we want to have a CSP absorber coating with total absorptance of the solar spectrum and total reflectance of the absorber's infrared radiation at an operating temperature as shown in Fig. 1 (ideal selective case). Real coatings show real selective behavior, such as the example (green) in Fig. 1. For a mid-temperature absorber, this represents a big advantage compared to non-selective coating, due to the high absorption of solar spectrum and high reflection of blackbody radiation at 573 K (applicable for LFR and PTC types).

On the contrary, at a high temperature of 1273 K, solar spectrum and blackbody spectrum overlap, so the α_S is the more important factor for ST and PD. Consequently, the ideal absorption–reflection transition wavelength of the coating is shifted to the higher wavelength, in order to absorb most of the solar spectrum (Fig. 1), and the highest ideal operational temperature for spectrally selective surface is reported to be 1273 K, which is 110 K lower than the ideal temperature for not spectrally selective absorbers [9]. Such a coating would still retain almost

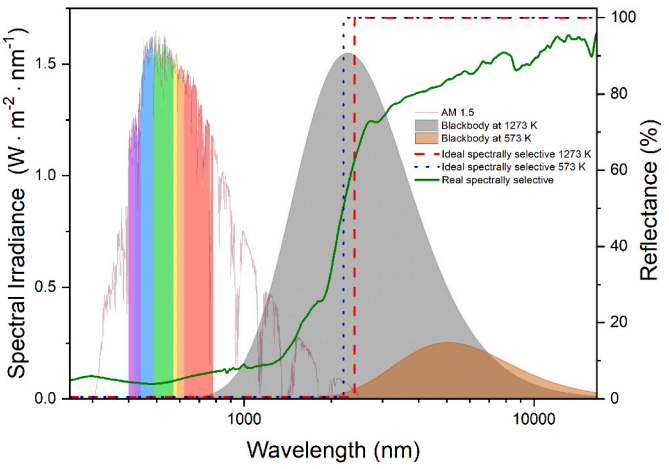

Fig. 1. Solar spectrum AM 1.5, blackbody emission spectrum at 573 K in gray (mid-temperature) and 1273 K in brown (high-temperature) on the bottom-left axis. The reflection spectra of an ideal spectrally selective coating for high- and mid-temperature CSP absorber and reflection spectrum of a real spectrally selective coating on the bottom-right axis. (For interpretation of the references to colour in this figure legend, the reader is referred to the Web version of this article.)

half of the absorber's infrared radiation at 1273 K, which would otherwise be lost to the environment (Fig. 1). Theoretically, a maximum efficiency of 65% is possible for a CSP plant with real selective absorber according to the study of Vetter et al. [9].

At higher temperatures (e.g., 1273 K), increased overlapping of solar spectra and the absorber's infrared emission spectra occurs (see Fig. 1), and therefore, it is possible to achieve high FOM with a high solar absorptive (HSA) coating.

However, at a sun concertation factor exceeding 100 suns and temperatures up to 1273 K, the ideal transition wavelength is 2.4 μm. Since there are not many materials with the required optical properties and long term-durability at such conditions, the research for the best absorber coating is still on-going. Therefore, to support future research and development of spectrally selective coatings (SSCs), we conducted a review of the CSP absorber coatings produced and reported to date.

2. Solar-to-thermal energy conversion efficiency

The FOM for low C and mid-temperature absorbers (Fig. 2a) and for high C and high-temperature absorbers (Fig. 2b) were calculated from eq. (4). The first scenario (Fig. 2a, black symbol graph) predicts a not spectrally selective absorber with a constant high ε_T of 0.9, but the α_S is changed from 0.6 to 1 to see the effect on the FOM. The second scenario (Fig. 2a, red symbol graph) predicts a spectrally selective coating with a constant high α_S of 0.95, but ε_T is changed from 0 to 1.

It is seen in Fig. 2 that at C = 10 and T = 573 K, increasing the α_S for non-selective coating results in a slower increase in FOM in contrast with lowering the ε_T for selective coating, where much higher FOM can be achieved. Furthermore, for C = 1000 and T = 1273 K, increasing the α_S for non-selective coating results in higher inclination (Fig. 2b, black symbol graph) and higher maximal FOM, while lowering the ε_T for the spectral selective case has a lesser effect on FOM for high C and T,

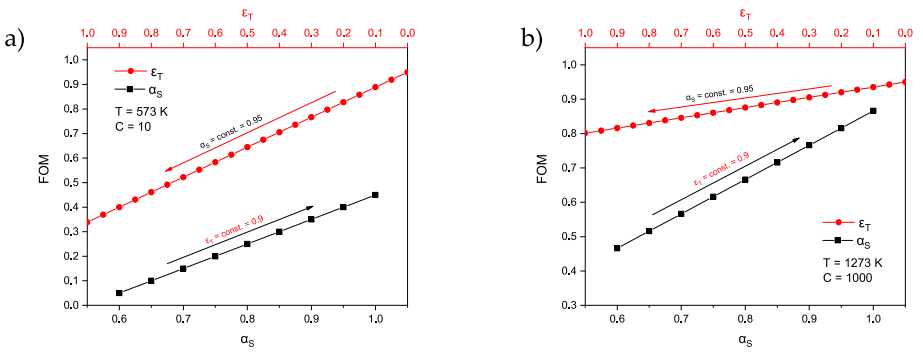

Fig. 2. Comparison of the FOM of a not spectrally selective coating with the α_S changing from 60% to 100% (black symbol graphs) at a constant ε_T with the FOM of a spectrally selective coating with ε_T changing from 100% to 0% at a constant high α_S (red symbol graphs). Graph (a) is calculated for the low concentration factor C = 10 and mid-temperature T_{abs} = 573 K and (b) is for the high concentration factor C = 1000 and high-temperature T_{abs} = 1273 K. (For interpretation of the references to colour in this figure legend, the reader is referred to the Web version of this article.)

although higher maximal FOM can be achieved. Increasing the CSP absorber operating temperatures above 1273 K would result in even less importance of spectral selectivity, and high solar absorptive (HSA) coating would be a reasonable choice to use in such case [9].

3. Spectrally selective absorber coating manufacturing methods

In this section, we describe some of the methods that are used for production of various SSC types. It is important to mention that the thickness of SSC (layers) plays an important role in achieving optimal thermal emittance values. Different methods offer different thickness adjustment options.

3.1. Spray coating

Spray coating is based on the formation of tiny droplets (atomization), which are transformed back into a smooth film when they are deposited in the substrate. Atomization can be achieved pneumatically [11–19] or hydraulically by centrifugal forces or by electrical forces [20]. Electrostatic spray coating can achieve up to 98% of material yield, but pneumatic spray coating is far less efficient, sometimes below 40%. Increasing parameters such as paint flow, viscosity of paint and surface tension will increase the droplet size in a spray, but increasing the density of paint and air flow will decrease the droplet size.

3.2. Spray pyrolysis

Spray pyrolysis is a thin film fabrication process, which involves transformation of a metal salt solution into micro sized droplets, which are sprayed onto the heated substrate, where they form the shape of a disk [21–24]. This is followed by the solvent evaporation, thermal decomposition and conversion of metal salt into oxides [25]. The most important parameter of spray pyrolysis is the substrate temperature, which determines the microstructure of the film that can form cracks, pores or dense material.

3.3. Dip coating

Dip coating is a wet chemical thin film deposition process that consists of immersion of the substrate into the precursor solution followed by a dwell time to allow sufficient time for the complete wetting of the substrate [26–31]. After that, the substrate is pulled out from a solution at a constant speed for the deposition of a uniform film. Finally, the solvent evaporates from the fluid for the formation of a thin film. Additional heat treatment can accelerate evaporation, remove organic residues and induce crystallization of the oxides [32].

3.4. Spin coating

Spin coating is used for rapid deposition of thin films on flat substrates [33–35]. The solution to be deposited is usually dispensed in the middle of the substrate and the spinning motion of the substrate causes the solution to spread out, leaving behind a uniform thin coating [36]. Dispense can be static before the rotation or dynamic during the rotation. The final film thickness is controlled by viscous flow and evaporation of the solvent. Longer spin times and higher spin speed result in a thinner film.

3.5. Laser sintering

Laser sintering is a process that allows surface sintering of the coating without overheating or oxidizing the substrate. Moreover, sintering runs in a scanning mode, where many parameters can be controlled, including pulse frequency, speed, energy density, laser wavelength, spacing between the scans, scanning repetitions and the atmosphere [17,37,38]. Laser technology besides sintering also enables the formation of laser-induced periodic surface structures (LIPSS), useful for the development of textured spectrally selective surfaces [39].

3.6. Chemical vapor deposition

Chemical vapor deposition or CVD is used to produce coatings where most metals can be used as well as silicon, carbon and compounds such as carbides, nitrides, oxides, etc. CVD is the deposition of a solid on a heated surface from a chemical reaction in the vapor phase, where deposited species are atoms or molecules [40]. The advantages of CVD are its ability to cover 3D structures, recesses and holes on the substrate and a high rate of deposition [41–44]. It does not require high vacuum and it is possible to change the precursor composition during deposition. The disadvantages are a high operating temperature of 600 °C and high vapor pressure of precursors, which can be hazardous or extremely toxic.

3.7. Atomic layer deposition

Atomic layer deposition or ALD is an upgraded variation of CVD. Usually with CVD, a mixture of reactants in a vapor phase is introduced into the deposition chamber. The difference with ALD is that initially, only one reactant is introduced, deposited to the substrate and then pumped out. Then, another reactant is introduced, which reacts with the monolayer of the first reactant, adsorbed to the surface, forming one layer of a solid film with the reaction product composition. The process can be repeated many times to obtain the desired thickness [45–52]. The advantage of ALD is that reactants cannot react in the vapor phase, which results as a film with embedded solid particles [53].

3.8. Physical vapor deposition

Physical vapor deposition or PVD is similar to the CVD atomistic deposition process in which a material is vaporized from a solid or a liquid source. The vapor is in a vacuum or a low-pressure gas or plasma and transported to the substrate, where it condenses to form a thin film

in a thickness range from few nanometers to few micrometers [52, 54–60]. Typical deposition rates are 1–10 nm per second. PVD processing can be divided into four categories: vacuum deposition, sputter deposition, arc vapor deposition and ion plating [61].

Pulsed laser deposition (PLD) is a vacuum deposition method, where a laser is used to vaporize surfaces and highly directed vapors can be ionized by laser radiation. These vapors provide the material to be deposited on a substrate to form a thin film. PLD was proven to be effective for deposition of multicomponent inorganic epitaxial thin films. The advantages of PLD are the stoichiometric transfer of the material from the target, the generation of energetic species, the hyperthermal reaction between ablated cations and the background gas in the ablation plasma, as well as compatibility with background pressures ranging from ultrahigh vacuum to 133 Pa [62].

3.9. Electroless plating

Electroless plating is an autocatalytic chemical deposition method, where a metal is deposited from an aqueous solution with a redox reaction [63–65]. No external electrical power source is used; the electron source is a reducing agent in the solution. The simplest form of plating is a metal displacement reaction, where less noble metal atoms dissolve and are replaced by atoms of a more noble metal from the solution. The reaction involves electron transfer between reacting chemical species [66,67].

3.10. Electroplating

Electroplating of metals and alloys uses an external power supply to provide the electrons for the reduction of metal ions to be deposited on a metal electrode from aqueous, organic and fused-salt electrolytes [68–70]. The reduction reaction can be described as:

$$M^{z+} + ze^{-} = M_{lattice}$$

The electroplating process is dependent on metal–solution interface properties, kinetics and mechanism of deposition, nucleation and growth process of the metal lattice and the structure and properties of the deposits [71–80].

3.11. Lithography, etching

Photolithography or optical lithography is used to selectively remove parts from a thin film or the bulk of a substrate. By spin coating, the substrate is first coated with a thin film of photoresists. Using UV light, projected through a mask onto the photoresist film, the exposed area is changed and exposed or not exposed area can be selectively removed, leaving a pattern on the substrate [50,81,82]. In optical lithography, resolution is determined by the diffraction of light. Currently, the resolution limit of optical lithography is at 193 nm [83].

Because of the industrial need for lower resolution, nanoimprint

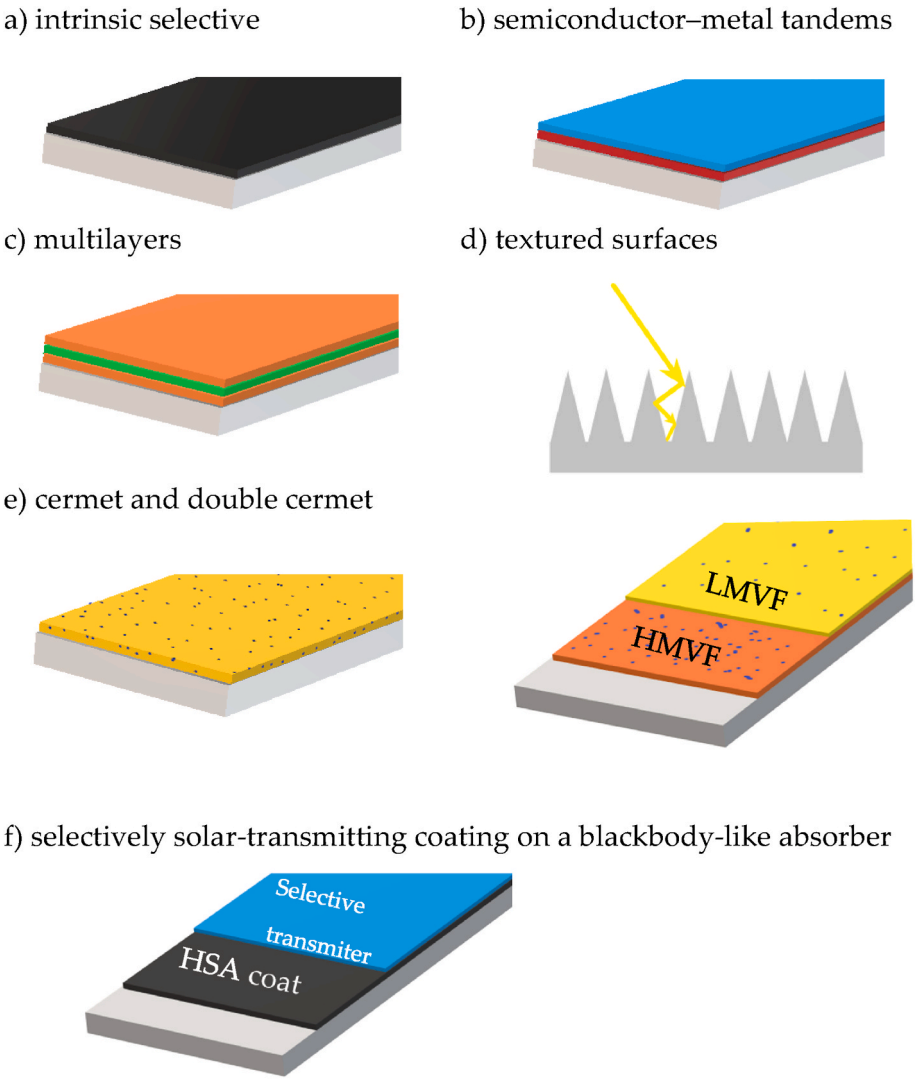

Fig. 3. Schematic representation of the different design types for the fabrication of spectrally selective coatings.

lithography was developed, which has a resolution limit below 5 nm [81]. The process consists of three steps: (1) mold fabrication, (2) imprint process and (3) subsequent etching.

In research, PVD is the most commonly used method to produce SSCs for CSP absorbers. Its advantage is in high control over deposition parameters and wide choice of precursor materials, which offer fabrication of well-defined compositions at nanoscale. Despite of higher production cost, PVD is already used at industrial level for mid-temperature PTC absorbers [84]. These coatings currently offer the highest solar-to-thermal efficiency in the CSP market. However, they are not yet stable enough to be used at high temperatures in air, mainly due to poor resistance to interlayer diffusion and oxidation, which causes mechanical and optical degradation of the coatings [85] [–] [88]. PVD can be used to produce all types of coatings described in Fig. 3.

Next, second most commonly used methods of deposition are more conventional and low-cost, e.g. spray coating, dip coating and spin coating, which deposit materials dispersed or dissolved in solvents and need subsequent curing to form a solid coating. They are usually used to deposit composite coatings. With these methods it is possible to achieve higher long-term stability at high temperatures. Since less control is possible over deposition process, these methods are suitable to produce thicker coatings with high solar absorptance, but they also have higher thermal emittance in comparison to PVD coatings (Table 2) [89,90].

4. Spectral selectivity and thermal stability of SSC

One of the first reports on spectrally selective coatings is a patent by Tabor from 1955, which is about a spectrally selective absorber for solar energy collectors [91]. He discovered that anodizing a bright nickel surface creates a thin film of dark nickel with α_S of 0.8 and ε_T of 0.12, with good thermal stability at 400 °C.

There were many material designs developed with the purpose of achieving the outstanding spectral selective properties of solar absorber coatings. The most important among them are intrinsic selective materials, semiconductor–metal tandems, multilayers, multi-dielectric composites, textured surfaces and a selectively solar-transmitting coating on a blackbody-like absorber [92]. Nanostructured metamaterials [93] and photonic crystals [94] can be considered as a subclass of textured surfaces.

4.1. Intrinsic selective materials

Intrinsic selective materials can have a suitable spectral selectivity, even 0.15 of ε_T/α_S ratio, but they do not have high enough α_S ($\geq$0.95) and are thus uncompetitive with other SSC types. Some of them also lack thermal oxidation resistance in air, despite of having high melting temperatures. However, the use of these materials for the fabrication of structured or composite coatings could increase their spectral selectivity.

4.2. Semiconductor–metal tandems

The semiconductor part of a tandem coating has the function of high solar absorption, which is dependent on a semiconductor bandgap. The metal part of a tandem has a property of low ε_T to reduce thermal losses. Semiconductor–metal tandem coatings can achieve very high α_S up to 99%, but are not thermally stable at high temperatures in air for longer time periods.

4.3. Multilayers, multi-dielectric composites

Multilayer absorber coatings consist of multiple thin layers, which can have antireflective, dielectric, metal, IR reflective, solar absorptive and other optical properties. With this kind of coating, it is possible to manipulate the optical properties in many ways and achieve both high solar absorptance and low thermal emittance. The disadvantages of such coatings are the high cost of fabrication and, similarly to tandem coatings, they are not stable at high temperatures for longer periods.

4.4. Textured surfaces

Surface texturing increases the number of reflections of incident light, leading to higher solar absorption. It is reported that the nanostructures on the surface act as a trap for light, which reflects inside of them many times until it is absorbed. The structures can be of different shapes and sizes. With textured surfaces, it is possible to achieve high α_S of 95% and low ε_T of 5%, but long-term thermal stability is not yet reported for them.

Photonic crystals can be classified as a special type of textured surfaces. These are periodic optical structures that can control the flow of light. Multiple reflections from surfaces separated by a distance similar to the wavelength prevent an optical beam from propagating through the crystal. Therefore, photonic crystal devices can force light around sharp bands or even trap it entirely [95].

4.5. Metal/metal compound–dielectric composite

Metal dielectric composite or cermet has a ceramic matrix with embedded metal particles. In the UV/VIS wavelength range, the composite has ceramic properties with high α_S and in IR wavelengths, it has metallic properties with low ε_T. High α_S can be achieved with smaller particle size and thicker coatings, whereas increasing the particle size decreases α_S. Thermal emittance can be lowered by decreasing the coating thickness and increasing the concentration of embedded metal particles [96].

Cao et al. report on double cermet coating deposition, which consist of two layers; the top layer has low metal volume fraction (LMVF) and bottom layer has high metal volume fraction (HMVF). The top layer contributes to high α_S and the bottom layer to low ε_T of the coating. Instead of pure metal particles, they used TiN embedded in SiO_2 to fabricate a composite [97].

High-temperature resistant paints can be considered a subclass of this category, where inorganic pigment nanoparticles, which can be metallic oxides, are embedded in a ceramic binder, forming a pigment–ceramic composite.

4.6. A selectively solar-transmitting coating on a blackbody-like absorber

This design combines a high solar absorptive coating (e.g., black paint) with a solar selective transmitter coating on top. Selective transmitter thin films can be made of different types of materials. One category is dielectric/metal/dielectric stacks, where TiO_2, ZnS and Al_2O_3 can be used as dielectrics and metals such as Ag, Au, Cu, Al.

Another category of candidates for thin film solar selective transmitters contains low energy band gap oxides of In, Sn, Cd and Zn, which are doped with elements such as Sb, F, Sn, B, Al, etc.

5. Thermal aging and long-term stability characterization of the industry CSP absorber coatings

After excellent optical properties (high α_S, low ε_T) of a CSP absorber coating are achieved, service lifetime is the next important property to consider. Factors affecting the service life of a coated CSP absorber are resistance against diffusion of the species from a substrate to a coating and/or vice versa; resistance against oxidation when the absorber is exposed to air; resistance against corrosion due to morning dew, acid rain, chlorides in the air moisture, if a plant is located close to the sea, etc.

Furthermore, rapid heating and cooling due to day and night cycles and thermal shocks due to cloud shading strongly affect the physical stability of the CSP absorber. When considering these facts, several studies have been carried out to assess long-term stability and service

Table 2
Types of spectrally selective coatings, differentiated by design, substrates and deposition method used, and the results of optical and thermal stability characterization [37,49–51,67,85,87–89,93,97,107,108,111–182].

Material	Substrate	Preparation Method	α_S	ε_T	Thermal Stability (°C)		Ref.
					Air	Vacuum	
Intrinsic Selective							
W	SS	Laser sintering	~0.90	0.49 (650 °C)	650 (36h)	-	[37,111]
MoO_3-doped Mo	Mo	CVD	0.74	< 0.30 (r.t.)	-	-	[112]
HfC	SS	PVD	0.925	0.13 (r.t.)	800	-	[113]
ZrB_2	SS	PVD	0.76	0.11	-	500 (100h)	[114]
SnO_2	Al	Pyrolytically	0.91	0.16	450	-	[115]
Co_3O_4	SS	Spray pyrolysis	0.93	0.14 (100 °C)	300	-	[116]
TaB_2	-	Hot pressing	0.7	0.3 (777 °C)	-	1200	[117]
MoO_3	Mo	Wet chemical etching	0.89	-	-	-	[118]
Semiconductor–Metal Tandem							
Si	Steel	PVD	0.70	0.17	570	-	[119], [120]
Ge	Steel	PVD	0.98	0.48	-	-	[119]
PbS	Steel	PVD	0.99	0.42	-	-	[119], [121], [122]
Cu_2S	Al	Spray pyrolysis	0.89	0.25	-	-	[123]
MWCNTs	Al	Electrophoretic deposition	0.91	0.20	500 °C	-	[124]
Multilayer Absorber							
Ag-TiO_2/ TiO_2/ SiO_2/ TiO_2/ SiO_2/	SS 321	Dip coating	0.94	0.11 (400 °C)	-	390	[125]
TiN/AlCrSiO	SS and Si	Cathodic arc ion plating	0.923	0.161	650 (200h	-	[126]
Cu/Al_2O_3/Cr/SiO_2/Cr/SiO_2	K9 glass or Si	PVD and ALD	0.954	0.196 (500 °C)	-	500 (72h)	[51]
Cr/CrAlN/CrAlON/CrAlO	SS	Cathodic arc ion plating	0.922	0.144	500 (1000h)	-	[127]
Al/$CrN_{0.95}$/$Cr_{0.96}Al_{0.04}N_{1.08}$/$Cr_{0.53}Al_{0.47}N_{1.12}$/$Al_2O_3$ and $Cr_{0.96}Al_{0.04}N_{1.08}$/$Cr_{0.62}Al_{0.38}N_{1.00}$/$Cr_{0.53}Al_{0.47}N_{1.12}$/$Al_2O_3$	Steel 316 L	HiPIMS	0.94	0.12	600 (2h)	-	[128]
AlCrMoTaTiN/Al_2O_3	SS	RF reactive magnetron sputtering	0.929	0.082	300	500 (2h)	[129]
W/AlSiTiNx/SiAlTiOyNx/SiAlOx	Glass, p-doped Boron Si, AISI304	PVD	0.95	0.01	500 (350h)	630 (220h)	[130]
W/WAlN/WAlON/Al_2O_3	SS	PVD	0.95	0.08	500 (150h)	-	[131]
TiC-TiN/Al_2O_3	SS	PVD	0.92	0.11	-	500 (100h)	[132]
Ti/AlN/Ti	SS 316L	PVD	0.89	0.19	-	-	[133]
AlCrTaTiZrN/SiO_2	SS and Si	PVD	0.965	0.086	-	600 (10h)	[134]

AlCrTaTiZrN	SS	PVD	0.93	0.15	-	600 (300h)	[135]
AlCrWTaNbTiN	SS	PVD	0.93	0.07	-	600 (240h)	[136]
TiB_2/Ti(B,N)/SiON/SiO_2	SS 304	PVD	0.981	0.15	400 (2h)	500 (250h)	[85]
Ti/TiB_2/Ti(B,N)/SiON/SiO_2					450 (2h)		
W/CrAlSiN_x/CrAlSiO_yN_x/SiAlO_x	SS	PVD	0.95	0.10	400 (650h)	600 (650h)	[137]
TiAlN_x/TiAlN_y/Al_2O_3	SS	PVD	0.93	0.22	550	-	[138]
Ti/TaC/Al_2O_3	SS	PVD	0.96	0.15	-	500	[139]
Mo/Al_2O_3	SS	PVD	0.90	0.08	350	600	[86]
ZrB_2/Al_2O_3	SS	PVD	0.92	0.11	-	500	[114]
TiB_2/Al_2O_3	SS	PVD	0.93	0.11	-	600	[140]
Cr/AlCrN/AlCrNO/AlCrN/AlCrNO/AlCrO	SS	PVD	0.90	0.15	500	-	[141]
TiAlC/TiAlCN/TiAlSiCN/TiAlSiCO/TiAlSiO	SS	PVD	0.96	0.07	325	650	[142]
SiO_2/Si_3N_4/W/SiO_2	W	CVD/PVD	0.95	0.10	600	-	[143]
HfO_x/Mo/HfO_2	SS	PVD	0.90	0.17	400	600	[144]
TiAl/TiAlN/TiAlON/TiAlO	SS	PVD	0.90	0.19	650 (1h)	-	[145]
WAlN/WAlON/Al_2O_3	SS	PVD	0.92	0.11	500 (2h)	-	[88]
SiO_2/AlN/$Ti_{1-x}Al_xN$/AlN/Pt	SS	PVD	0.92	0.15	-	900 (3h)	[146]
Mn-Cu-Co-Ox-ZrO_2/MgF_2	SS 304	Dip coating	0.93	0.20	700 (2h)	-	[147]
TiAlO/TiAlON/TiN	SS	Cathodic arc evaporation	0.92	0.18	550 (50h)	-	[148]
TiN/TiNxOy/SiO_2	Al	PVD	0.92	0.06	400 (240h)	-	[149]
TiC–ZrB_2/ZrB_2/Al_2O_3	SS	PVD	0.92	0.10	-	500 (100h)	[150]
NiP/TiO_2	1050 Al	Electroless plating	0.99	0.21	-	-	[67]
W/WAlSiN/SiON/SiO_2	SS	PVD	0.96	0.10	-	600 (200h)	[151]
TiNxOy/TiO_2/Si_3N_4/SiO_2	Cu, Si	PVD	0.98	0.45	-	-	[152]
$Ni_xCo_{3-x}O_4$/SiO_2	SS	Dip coating	0.94	0.18	500	-	[153]
HfB_2/Al_2O_3	SS, Si	PVD	0.92	0.11	500 (100h)	500 (100h)	[87]
TiC–ZrC/Al_2O_3	SS	PVD	0.92	0.13	400 (5h)	700 (100h)	[154]
Ti/Al_2O_3/MWCNTs	SS	PVD	0.95	0.20	-	-	[155]
$MoSi_2$–Si_3N_4/Si_3N_4/Al_2O_3	SS	PVD, ALD	0.92	0.46 (600 °C)	600 (2900)	-	[49]
Metal–Dielectric Composite							
Matrix	Insert						
Al_2O_3	W	SS or Si(100)	PVD	0.93	0.12	-	600 (10h)	[156]
	Ni	SS	PVD	0.94	0.07	500	-	[157]
	W			0.939	0.012	-	580	[158]
	Ag	Cu, Si, glass	PVD	0.89	0.06 (82 °C)	-	400 (2h)	[159]
	W-Ni	SS	PVD	0.90	0.15	600 (148h)	-	[160]
AlN	Ni-Cr	Glass	PVD	0.92-0.96	0.10 (350 °C)	-	-	[161]
Cr_2O_3	Cr	Ni	Electroplating	0.96	0.35	450		[162]
SiO_2	Mo	SS	PVD	0.95	0.15 (400 °C)	-	600	[163]
	Ni-B	SS	Dip coating	>0.80	<0.60	500	-	[164]
	TiN	LAO	PVD	0.94	0.08	-	700 (7d)	[97]
YSZ	W-Ni	SS	PVD	0.91	0.13	-	600	[165]
MgF_2	Ni-Cr	SS	PVD	0.96	0.05	-	-	[166]
Non-Metal–Dielectric Composite								
SiO_2	$CuCr_2O_4$	Haynes 230	Spray coating	0.97	0.91	800 (2000h)	-	[89]
	$Cu_{0.86}Cr_{0.14}Mn_{1.5}Fe_{0.5}O_4$	Inconel 617		0.97	0.86	800 (1300h)	-	[167]
	$Cu_xCo_{3-x}O_4$ $Cu_xMn_{3-x}O_4$	Inconel 625		>0.95	-	750 (1000h)	-	[168]
SiO_2/Al_2O_3	MWCNTs	Al		0.985	0.901	350 (100h)	-	[18]

SiO_2	MWCNTs	SS, Cu, Ni, Cr	Ultrasonic spraying/dip coating	0.92	0.22 (400 °C)	-	400	[169]
SiO_2	$MnFe_2O_4$	SS 310	Spray coating	0.93	0.52	750 (700h)	-	[107]
SiO_2	$TiSi_2$	SS		>0.90	<50	750 (1000h, on silica substrate)	-	[108]
Textured Surface								
Co_3O_4		Glass, Cu	PVD	0.965	0.035	-	-	[170]
Ti (gratings)/MgF_2/W		Si	e-beam evaporation and lithography	0.90	0.2	350	-	[171]
Ni (nanopyramids)		Ni	Template stripping	0.95	0.10	-	800	[172]
$Si_{0.8}Ge_{0.2}$ (nanostructures)		SS	Spark erosion	0.90	0.30	750 (1h)	-	[93]
TiAlN		Inconel 625	Spin coating	0.95	0.38	500 (444h)	-	[173]
Ag-CuO		SS-304	Dip coating	0.92	0.05	-	-	[174]
W		SS	PVD	0.90	0.06	-	-	[175]
Mo/Al_2O_3		SS 304	PVD	0.90	0.08	-	-	[176]
W 2D		W	Lithography, etching	0.90	0.3	/	/	[177]
Ta-W		Ta3%W	RIE	>0.80	<0.30	/	1200 (24h)	[178]
Ta		Ta	UV-NIL	0.96	0.46	-	-	[179]
Rh, HfO_2		Si	Lithography, ALD	0.85	0.10	1000 (24h)	-	[180]
Re_xNi_{100-x}		W	Self-assembly	0.90	0.50	1000 (5h)	-	[181]
W, HfB_2		Si, sapphire	ALD	>0.80	<0.40	-	1400	[182]
Pt, Al_2O_3		W (polyc.)	Lithography, ALD	0.92	0.18 (400 °C)	-	700	[50]

life of CSP absorber coatings, which are important contributions both to technical development and to the levelized cost of electricity (LCOE) estimation [98].

Extensive research with service-life predictions of isothermal and cyclic thermal loads on industrial high solar absorptive (HSA) coating deposited on Inconel 617 substrate was published by our group in 2019 [99]. The duration of the isothermal load was more than 3500 h at three different temperatures, 730, 750 and 770 °C, in an air furnace. An additional isothermal test at 750 °C with increased oxygen concentration was carried out in parallel to accelerate substrate oxidation.

Regarding cyclic conditions, three different peak temperatures, 530 °C, 640 °C and 700 °C, were chosen with a heating rate of either $r_1 = 8$ °C/min or $r_2 = 12$ °C/min. Additional cyclic tests were conducted with the furnace purged with steam when, after each cycle, the samples cooled down to room temperature to simulate morning dew precipitation at the industrial site. Each week, samples were taken from the furnace to perform the coating characterization, which involved crack length and width evaluation, pull-off testing, evaluation of the oxide thickness, determination of the spectral selectivity and XRD, FIB and TEM analysis.

Data from the absorptivity measurements, the crack length and width, the oxide thickness, the ratio between the oxide and the coating thickness and the pull-off results were used to develop theoretical models for the oxide growth rate and solar absorptance degradation, resulting in the service life estimation of the absorber coating studied, which was estimated to be 11 ± 2 years under the operating conditions. To calculate the estimation accurately, isothermal and cyclic data were merged, which gave the estimation of the lifetime. Furthermore, optical and mechanical degradation were considered separately to determine which is more progressive to reach the threshold value, and optical degradation was found to be dominant.

The recent review by Zhang et al. [100] on the thermal stability of high-temperature solar absorber coatings report the diffusion process as the main concerning issue. They divided diffusion into outer diffusion of oxygen, which oxidizes the substrate, and inner diffusion, which is divided further into internal segregation and internal penetration. The latter is reported to be the main reason for coating failure.

Pyromark 2500 can be considered as an industrial standard coating, which is used on high-temperature CSP absorbers. However, as seen from Fig. 2, due to its non-selective nature, Pyromark is not suitable for low-temperature absorbers. Too high thermal emissivity at a low temperature results in very low solar-to-thermal conversion efficiency (<40%). For this reason, other fabrication methods (PVD, CVD, ALD, electroplating, etc.) and materials are used to produce industrial PTC absorber coatings with high spectral selectivity, i.e., electroplating of Co–Cr coatings by Absolicon [101] or PVD-fabricated Ti/Cr/AlTiN/AlTiON/AlTiO multilayer coatings by Rioglass [102].

Boubalt et al. developed the LCOE metric to characterize industrial absorber coatings for CSP [103]. They also introduced two new parameters: LCOC (levelized cost of coating) and LCOC efficiency. Their estimation of coating reapplication intervals was from one to five years and their finding was that SSC absorber coatings could reduce the LCOE by up to 12%, compared to the value obtained for an uncoated absorber.

The properties of Pyromark 2500 are used by many authors as a comparison to newly developed absorber coatings. Ho et al. characterized Pyromark 2500 used as a solar absorber coating at a high temperature [104]. They reported that the coating achieved α_S of 0.97 at a near-normal incidence angle and ε_T of 0.8 at 100 °C. However, exposure of the coating to 750 °C (300 h) caused a drop in the α_S of 3%. The cause for the drop was stated to be high temperature-induced crystal structure change and/or diffusion of cations from the substrate into the coating.

Another more recent study about degradation mechanisms of

Pyromark 2500 was published by Torres et al. [7], where non-linear thermal cycling effects were considered in the study. Rapid cycling, cycle-and-hold and isothermal (850 °C, 100 h) experiments were conducted on the Inconel 625 samples, coated with Pyromark 2500. The results showed that cycle-and-hold conditions significantly differed from isothermal and rapid cycling cases, resulting in larger crack widths due to sintering and oxidation of the substrate. Furthermore, Ni and Cr diffusion from the substrate was observed, forming spinel structures.

Furthermore, despite the intensive research and development of new solar absorber coatings, there is still no commercial substitute for Pyromark paint for high-temperature applications [105]. For this reason, Martinez et al. studied means of improving the durability of Pyromark 2500 by controlling consolidation procedures. In their experiments, Pyromark-coated T22 substrates were exposed to different oven temperatures and times. Subsequently, polymerization was induced by infrared radiation, using different radiation powers and exposure times. The results showed that the thickness of the paint and substrate was not affected by thermal treatments. Local wear rate analysis was used to assess paint durability and relaxation function was measured with depth sensing indentation. The correlation between relaxation times, wear rate, the (hardness)^2:(equilibrium modus after relaxation) ratio and the glass transition temperature (T_g) was formed. It was found that the T_g and relaxation times can be controlled by strategic curing and vitrification procedure, and it was proposed that Pyromark be cured for 2 h at 125 °C followed by vitrification for 1 h at 250 °C.

Reoyo-Prats et al. studied accelerated ageing of absorber coatings for CSP absorbers under real high solar flux with high rates of flux (350 kW/m^{2}s to 640 kW/m^{2}s) and temperature variation [106]. In their study, T91, T22, VM12 and Inconel 617 alloys were coated and tested with 200 accelerated solar ageing cycles using a concentrated solar facility (SAAF) under two different cycle regimes. In the first regime, the samples were exposed to a concentrated solar flux of 500 kW/m^2 and a maximal temperature of 650 °C, and in the second regime, to a flux of 700 kW/m^2 and T_{max} of 800 °C.

After 200 cycles, there was no significant degradation of the samples. In some cases, thermal cycling even resulted in improved α_S of the coating, resulting in higher optical efficiency, such as for the coated T22 sample and the coated VM12 sample, due to a curing phenomenon. It was concluded that 200 cycles were insufficient to observe a higher degree of coating degradation.

The rapid progress in the spinel oxide pigmented silicone coatings for high-temperature CSP absorbers operating under high solar concentration was reported by X. Wang et al. [107–109] They used a four-flux radiative theoretical model in order to predict the optical properties of nano particle pigmented coatings. The theoretical results were a good match with an experimental absorber coating containing small load of spinel oxide nanoparticles. They achieved α_S of 93% and ε_T of 52% with $MnFe_2O_4$-pigmented coating on stainless steel 310. Furthermore, absorber coatings were isothermally aged for 1000h at 750 °C in air with subsequent 19 day-night thermal cycling. The results of aging showed the drop of α_S to 90.8% and increase of ε_T to 57.6%, but the optical degradation was mainly due to the CrOx microflake formation from the SS 310 substrate thermal oxidation rather than the coatings itself [107]. With a proper substrate oxidation protection, these absorber coatings are shown to be good candidates for high-temperature Generation 3 CSP systems [110].

Table 1 contains an overview of spectrally selective coatings with used fabrication methods, substrates, α_S and ε_T values and thermal stability in air and/or vacuum. State-of-the-art CSP-TR coatings can quickly achieve a high solar absorptance greater than 95%, but according to our literature review, coatings for CSP-TR systems that provide a low thermal emittance (<50%) over a long period of time (1000 h) at temperatures of 700 °C or higher in the air have not been reported.

The α_S with a threshold of 95%, ε_T with values lower than 50% and 1000 h of isothermal stability or cycle equivalent testing in an air atmosphere of CSP absorber coatings were chosen from Table 2 and are summarized in Table 3. One can observe that only metal/non-metal–dielectric composite coatings achieve high spectral selectivity and long-term high-temperature stability in the air, but even these coatings usually do not have both features. Other coating designs report insufficient thermal stability for industrial use or, in the case of semiconductor–metal tandems, thermal stability was not reported, according to our knowledge. The threshold for high α_S as a more important factor was not achieved with the intrinsic and textured surface coating designs, but low ε_T, at least for as-deposited coatings, was reported for all design types. Despite the suitable initial optical properties of many fabricated coatings, they are not industrially feasible unless they show appropriate thermal and mechanical stability at operating conditions and low cost of large-scale fabrication.

Table 3
Assessment of reported optical properties and thermal stability, required for effective high-temperature CSP spectrally selective absorber coatings, which are arranged by design types.

Material type	$\alpha_S > 95\%$	$\varepsilon_T < 50\%$	Long-term thermal stability in air at T > 873 K (t > 1000 h) isothermally or cycle equivalent
Intrinsic selective materials	×	✓	×
Semiconductor–metal tandems	✓	✓	/
Multilayers, multi-dielectric composites	✓	✓	×
Metal/metal oxide-dielectric composite (cermet and double cermet)	✓	✓	✓
Textured surfaces	×	✓	×

6. Conclusions and future prospects

Absorber coatings are the key component in the solar-to-thermal energy conversion process. Six basic types of SSCs have been developed to date, with the aim of designing an efficient CSP absorber system. For low-to-mid temperature (<400 °C) applications, the choice of suitable materials for SSC production is larger, and thermal stability in air is easier to achieve in contrast to very high temperature (>800 °C) applications, for which some refractory materials could be the best candidates in order to achieve a degradation-resistant coating for a longer period of time (>10 years).

A spectrally selective coating can reduce the LCOE by up to 12% compared to an uncoated absorber [103]. In the case of producing heat for industry, the reduction in the levelized cost of heat production is even higher, since there is no loss of energy due to the transformation of heat to mechanical and electrical energy.

For temperatures higher than 1273 K, high FOM is possible with high solar absorptive (HSA) coating only, and spectral selectivity plays a minor role. More attention should be dedicated to the thermal conductivity of the absorber system and heat transfer coefficient of the heat transfer fluid boundary layer [183].

Among the fabrication methods for the production of spectrally selective absorber coatings, the emerging technologies are CVD and PVD and methods evolved from them. Due to higher LCOC in comparison with cheaper deposition methods (e.g., spray coating), there is always a search for the next best industrially feasible fabrication process. With PVD or CVD techniques and the right choice of materials and parameters of fabrication, it is possible to achieve very high α_S as well as extremely low ε_T of SSCs. However, the main weaknesses of all SSC types are chemical and physical degradation under high-temperature cycling conditions, which are present at the CSP absorbers under operation.

Degradation and high temperature-induced oxidation and diffusion result in the loss of excellent optical properties and demands reapplication or replacement, which increases the operating costs.

Future efforts should be focused on the lifetime assessment of the coatings with suitable spectral selectivity to choose the most stable coatings for further development into industrial applications operating either at low, medium or high temperatures.

Characterization methods should be used in a manner that approaches the real industrial absorber conditions as much as possible, and theoretical models should be developed and used to predict long-term degradation behavior [146].

CRediT authorship contribution statement

Luka Noč: Visualization, Conceptualization, Formal analysis, Investigation, Methodology, Writing – original draft. **Ivan Jerman:** Writing – review & editing, Supervision, Resources, Project administration, Funding acquisition.

Declaration of competing interest

The authors declare that they have no known competing financial interests or personal relationships that could have appeared to influence the work reported in this paper.

Acknowledgements

The authors acknowledge that the project Forthcoming Research and Industry for European and National Development of Solar Heat Industrial Processes (FRIENDSHIP, grant agreement no. 884213) was financially supported by the European Commission under the funding programme H2020-LC-SC3-2019.

References

[1] DESERTEC Foundation | Energy for the Next Billion, (n.d.). https://www.desertec.org/(accessed April 20, 2021).
[2] IRENA, OECD/IEA, REN21, Renewable Energy Policies in a Time of Transition: Heating and Cooling, 2020.
[3] Friendship, (n.d.). https://friendship-project.eu/. (Accessed 14 May 2021).
[4] Mapa-de-proyectos-Diciembre-2020.jpg (JPEG Image, 1031 × 433 Pixels), (n.d.). https://www.solarpaces.org/wp-content/uploads/Mapa-de-proyectos-Diciembre-2020.jpg (accessed February 15, 2021).
[5] B. Hoffschmidt, Receivers for Solar Tower Systems, 2014, 33, https://www.google.com/search?client=firefox-b-d&q=Receivers+for+Solar+Tower+Systems+Prof.+Dr.+Bernhard+Hoffschmidt, 31,2.
[6] N. El Gharbi, H. Derbal, S. Bouaichaoui, N. Said, A comparative study between parabolic trough collector and linear Fresnel reflector technologies, Energy Proc. 6 (2011) 565–572, https://doi.org/10.1016/j.egypro.2011.05.065.
[7] J.F. Torres, I. Ellis, J. Coventry, Degradation mechanisms and non-linear thermal cycling effects in a high-temperature light-absorber coating, Sol. Energy Mater. Sol. Cells 218 (2020), 110719, https://doi.org/10.1016/j.solmat.2020.110719.
[8] Power Tower, (n.d.). https://solarpaces.nrel.gov/by-technology/power-tower (accessed January 7, 2021).
[9] K. Burlafinger, A. Vetter, C.J. Brabec, Maximizing concentrated solar power (CSP) plant overall efficiencies by using spectral selective absorbers at optimal operation temperatures, Sol. Energy 120 (2015) 428–438, https://doi.org/10.1016/j.solener.2015.07.023.
[10] Y. Tian, X. Liu, A. Ghanekar, Y. Zheng, Scalable-manufactured metal–insulator–metal based selective solar absorbers with excellent high-temperature insensitivity, Appl. Energy 281 (2021), 116055, https://doi.org/10.1016/j.apenergy.2020.116055.
[11] G. Tagliabue, H. Eghlidi, D. Poulikakos, Rapid-response low infrared emission broadband ultrathin plasmonic light absorber, Sci. Rep. 4 (2014) 7181, https://doi.org/10.1038/srep07181.
[12] T.K. Kim, B. VanSaders, J. Moon, T. Kim, C.-H. Liu, J. Khamwannah, D. Chun, D. Choi, A. Kargar, R. Chen, Z. Liu, S. Jin, Tandem structured spectrally selective coating layer of copper oxide nanowires combined with cobalt oxide nanoparticles, Nano Energy 11 (2015) 247–259, https://doi.org/10.1016/j.nanoen.2014.10.018.
[13] P. Ma, Q. Geng, X. Gao, S. Yang, G. Liu, Spectrally selective Cu1.5Mn1.5O4 spinel ceramic pigments for solar thermal applications, RSC Adv. 6 (2016) 32947–32955, https://doi.org/10.1039/C6RA03300H.
[14] P. Ma, Q. Geng, X. Gao, S. Yang, G. Liu, CuCr2O4 spinel ceramic pigments synthesized by sol-gel self-combustion method for solar absorber coatings, J. Mater. Eng. Perform. 25 (2016) 2814–2823, https://doi.org/10.1007/s11665-016-2143-z.
[15] A.K. Saha, L. Chandra, A. Dixit, in: L. Chandra, A. Dixit (Eds.), Transition Metal-Based Spectrally Selective Coatings Using In-House Developed Spray System BT - Concentrated Solar Thermal Energy Technologies, Springer Singapore, Singapore, 2018, pp. 145–155.
[16] N. Selvakumar, G. Karthik, S. Jayaraj, H.C. Barshilia, Sprayable PEDOT:PSS based spectrally selective coating for solar energy harvesting, Sol. Energy Mater. Sol. Cells 221 (2021), 110906, https://doi.org/10.1016/j.solmat.2020.110906.
[17] X. Pang, F. Zhou, Thermostability and weatherability of TiN/TiC-Ni/Mo solar absorption coating by spray method-laser cladding hybrid deposition, Opt Laser. Eng. 127 (2020), 105983, https://doi.org/10.1016/j.optlaseng.2019.105983.
[18] R.K. Bera, Y. Binyamin, C. Frantz, R. Uhlig, S. Magdassi, D. Mandler, Fabrication of self-cleaning CNT-based near-perfect solar absorber coating for non-evacuated concentrated solar power applications, Energy Technol. 8 (2020), 2000699, https://doi.org/10.1002/ente.202000699.
[19] E. Maimon, A. Kribus, Y. Flitsanov, O. Shkolnik, D. Feuermann, L. Larush, D. Mandler, S. Magdassi, T. Aviv, E. Physics, B. Gurion, S.B. Campus, Wet-chemistry based selective coatings for concentrating solar power 8834, 2013, pp. 1–13, https://doi.org/10.1117/12.2025579.
[20] H.-J. Streitberger, A. Goldschmidt, BASF Handbook Basics of Coating Technology, 3rd Revised Edition, 2018.
[21] A. James, P. Pradeep, H. Barshilia, V.B. Kamble, Effect of surface roughness on the solar photothermal conversion efficiency of spray-coated CuCo2O4 films, J. Appl. Phys. 127 (2020), 145303, https://doi.org/10.1063/1.5143348.
[22] M. Voinea, E. Ienei, C. Bogatu, A. Duta, Solar selective coatings based on nickel oxide obtained via spray pyrolysis, J. Nanosci. Nanotechnol. 9 (n.d.) 4279–4284.
[23] S. Golshahi, A.B. Khatibani, S.M. Rozati, Microstructure and optical properties of spray-pyrolysed FeAlO x cermet as a spectrally selective solar absorber coating, J. Nanoelectron. Optoelectron. 13 (n.d.) 897–905.
[24] A. Cuevas, R. Romero, E.A. Dalchiele, J.R. Ramos-Barrado, F. Martin, D. Leinen, Spectrally selective CuS solar absorber coatings on stainless steel and aluminum, Surf. Interface Anal. 48 (2016) 649–653, https://doi.org/10.1002/sia.5971.
[25] V.K. Singh, Thin film deposition by spray pyroysis techniques, Emerg. Technol. Innov. Res. 4 (2017) 1–9.
[26] M.E. Rincón, J.D. Molina, M. Sánchez, C. Arancibia, E. García, Optical characterization of tandem absorber/reflector systems based on titanium oxide–carbon coatings, Sol. Energy Mater. Sol. Cells 91 (2007) 1421–1425, https://doi.org/10.1016/j.solmat.2007.04.005.
[27] S. Pal, D. Diso, S. Franza, A. Licciulli, L. Rizzo, Spectrally selective absorber coating from transition metal complex for efficient photothermal conversion, J. Mater. Sci. 48 (2013) 8268–8276, https://doi.org/10.1007/s10853-013-7639-4.
[28] M. He, R. Chen, Structural and optical properties of CuMnCoOx spinel thin films prepared by a citric acid-based sol–gel dip coating route for solar absorber applications, J. Sol. Gel Sci. Technol. 74 (2015) 528–536, https://doi.org/10.1007/s10971-015-3630-7.
[29] P. Ma, Q. Geng, X. Gao, T. Zhou, S. Yang, G. Liu, Aqueous solution-derived CuMn2O4 ceramic films for spectrally selective solar absorbers, Ceram. Int. 42 (2016) 19047–19057, https://doi.org/10.1016/j.ceramint.2016.09.062.
[30] S.R. Atchuta, S. Sakthivel, H.C. Barshilia, Nickel doped cobaltite spinel as a solar selective absorber coating for efficient photothermal conversion with a low thermal radiative loss at high operating temperatures, Sol. Energy Mater. Sol. Cells 200 (2019), 109917, https://doi.org/10.1016/j.solmat.2019.109917.
[31] M. Shiva Prasad, B. Sobha, K. Suresh, S. Sakthivel, Cu(Mn0.748Ni0.252)2O4/SiO2 nanoparticle layers for wide-angle spectral selectivity and high thermal stability, ACS Appl. Nano Mater. 3 (2020) 7869–7878, https://doi.org/10.1021/acsanm.0c01363.
[32] T. Schneller, R. Waser, M. Kosec, D. Payne, Chemical Solution Deposition of Functional Oxide Thin Films, Springer-Verlag Wien, 2016.
[33] T.K. Boström, E. Wäckelgård, G. Westin, Durability tests of solution-chemically derived spectrally selective absorbers, Sol. Energy Mater. Sol. Cells 89 (2005) 197–207, https://doi.org/10.1016/j.solmat.2005.01.014.
[34] Y. Liu, Z. Wu, L. Yin, Z. Zhang, X. Wu, D. Wei, Q. Zhang, F. Cao, High-temperature air-stable solar absorbing coatings based on the cermet of MoSi2 embedded in SiO2, Sol. Energy Mater. Sol. Cells 200 (2019), 109946, https://doi.org/10.1016/j.solmat.2019.109946.
[35] R.N. Abed, M. Abdallh, A. Adnan Rashad, H.C. Al-Mohammedawi, E. Yousif, Spectrally selective coating of nanoparticles (Co3O4:Cr2O3) incorporated in carbon to captivate solar energy, Heat Transf 49 (2020) 1386–1401, https://doi.org/10.1002/htj.21668.
[36] M.A. Aegerter, M. Mennig, Sol-gel Technologies for Glass Producers and Users, Springer, New York; London, 2011.
[37] A.A. Shah, C. Ungaro, M.C. Gupta, High temperature spectral selective coatings for solar thermal systems by laser sintering, Sol. Energy Mater. Sol. Cells 134 (2015) 209–214, https://doi.org/10.1016/j.solmat.2014.11.009.
[38] N. Li, D.-J. Yang, Y. Shao, Y. Liu, J. Tang, L. Yang, T. Sun, W. Zhou, H. Liu, G. Xue, Nanostructured black aluminum prepared by laser direct writing as a high-performance plasmonic absorber for photothermal/electric conversion, ACS Appl. Mater. Interfaces 13 (2021) 4305–4315, https://doi.org/10.1021/acsami.0c17584.
[39] P. Gregorčič, M. Sedlaček, B. Podgornik, J. Reif, Formation of laser-induced periodic surface structures (LIPSS) on tool steel by multiple picosecond laser pulses of different polarizations, Appl. Surf. Sci. 387 (2016) 698–706, https://doi.org/10.1016/j.apsusc.2016.06.174.

[40] H.O. Pierson, Handbook of Chemical Vapor Deposition : Principles, Technology and Applications, 2014.
[41] K. Niranjan, A. Soum-Glaude, A. Carling-Plaza, S. Bysakh, S. John, H.C. Barshilia, Extremely high temperature stable nanometric scale multilayer spectrally selective absorber coating: emissivity measurements at elevated temperatures and a comprehensive study on ageing mechanism, Sol. Energy Mater. Sol. Cells 221 (2021), 110905, https://doi.org/10.1016/j.solmat.2020.110905.
[42] D.D. Allred, M.R. Jacobson, E.E. Chain, Spectrally selective surfaces by chemical vapor deposition, Sol. Energy Mater. 12 (1985) 87–129, https://doi.org/10.1016/0165-1633(85)90027-9.
[43] A. Dan, H.C. Barshilia, K. Chattopadhyay, B. Basu, Solar energy absorption mediated by surface plasma polaritons in spectrally selective dielectric-metal-dielectric coatings: a critical review, Renew. Sustain. Energy Rev. 79 (2017) 1050–1077, https://doi.org/10.1016/j.rser.2017.05.062.
[44] C. Wang, W. Li, Z. Li, B. Fang, Solar thermal harvesting based on self-doped nanocermet: structural merits, design strategies and applications, Renew. Sustain. Energy Rev. 134 (2020), 110277, https://doi.org/10.1016/j.rser.2020.110277.
[45] M. Śmietana, M. Myśliwiec, P. Mikulic, B. Witkowski, W. Bock, Capability for fine tuning of the refractive index sensing properties of long-period gratings by atomic layer deposited Al2O3 overlays, Sensors 13 (2013) 16372–16383, https://doi.org/10.3390/s131216372.
[46] N. Jeon, I. Lightcap, D.J. Mandia, A.B.F. Martinson, Plasma-Enhanced atomic layer deposition of TiAlN: compositional and optoelectronic tunability, ACS Appl. Mater. Interfaces 11 (2019) 11602–11611, https://doi.org/10.1021/acsami.8b21461.
[47] S. Babar, A.U. Mane, A. Yanguas-Gil, E. Mohimi, R.T. Haasch, J.W. Elam, W: Al2O3 nanocomposite thin films with tunable optical properties prepared by atomic layer deposition, J. Phys. Chem. C 120 (2016) 14681–14689, https://doi.org/10.1021/acs.jpcc.6b03823.
[48] Z.-Y. Wang, R.-J. Zhang, H.-L. Lu, X. Chen, Y. Sun, Y. Zhang, Y.-F. Wei, J.-P. Xu, S.-Y. Wang, Y.-X. Zheng, L.-Y. Chen, The impact of thickness and thermal annealing on refractive index for aluminum oxide thin films deposited by atomic layer deposition, Nanoscale Res. Lett. 10 (2015) 46, https://doi.org/10.1186/s11671-015-0757-y.
[49] E. Céspedes, A. Rodríguez-Palomo, E. Salas-Colera, E. Fonda, F. Jiménez-Villacorta, M. Vila, A. de Andrés, C. Prieto, Role of Al2O3 antireflective layer on the exceptional durability of Mo–Si–N-based spectrally selective coatings in air at high temperature, ACS Appl. Energy Mater. 1 (2018) 6152–6160, https://doi.org/10.1021/acsaem.8b01183.
[50] M. Shimizu, H. Akutsu, S. Tsuda, F. Iguchi, H. Yugami, A high-temperature solar selective absorber based upon periodic shallow microstructures coated by multi-layers using atomic layer deposition, Photonics 3 (2016), https://doi.org/10.3390/photonics3020013.
[51] Y. Wu, E.-T. Hu, Q.-Y. Cai, J. Wang, Z.-Y. Wang, H.-T. Tu, K.-H. Yu, L.-Y. Chen, W. Wei, Enhanced thermal stability of the metal/dielectric multilayer solar selective absorber by an atomic-layer-deposited Al2O3 barrier layer, Appl. Surf. Sci. 541 (2021), 148678, https://doi.org/10.1016/j.apsusc.2020.148678.
[52] N. Selvakumar, H.C. Barshilia, Review of physical vapor deposited (PVD) spectrally selective coatings for mid- and high-temperature solar thermal applications, Sol. Energy Mater. Sol. Cells 98 (2012) 1–23, https://doi.org/10.1016/j.solmat.2011.10.028.
[53] T. Kaariainen, Atomic Layer Deposition : Principles, Characteristics, and Nanotechnology Applications, second ed., John Wiley & Sons, Hoboken, NJ, 2013.
[54] C.W. Chen, D.Y. Chen, C.Y. Hsu, Y.H. Chang, K.H. Hou, Spectrally selective Al/AlN/Al/AlN tandem solar absorber by inline reactive ac magnetron sputtering, Surf. Eng. 27 (2011) 616–622, https://doi.org/10.1179/026708410X12786785573436.
[55] C. Nunes, V. Teixeira, M.L. Prates, N.P. Barradas, A.D. Sequeira, Graded selective coatings based on chromium and titanium oxynitride, Thin Solid Films 442 (2003) 173–178, https://doi.org/10.1016/S0040-6090(03)00967-2.
[56] A.B. Khelifa, S. Khamlich, Z.Y. Nuru, L. Kotsedi, A. Mebrahtu, M. Balgouthi, A. A. Guizani, W. Dimassi, M. Maaza, Growth and characterization of spectrally selective Cr2O3/Cr/Cr2O3 multilayered solar absorber by e-beam evaporation, J. Alloys Compd. 734 (2018) 204–209, https://doi.org/10.1016/j.jallcom.2017.11.036.
[57] K. Valleti, S.G. Rao, P. Miryalkar, A. Sandeep, D.S. Rao, Cr-(CrN/TiAlN)m-AlSiN-AlSiO open-air stable solar selective coating for concentrated solar thermal power applications, Sol. Energy Mater. Sol. Cells 215 (2020), 110634, https://doi.org/10.1016/j.solmat.2020.110634.
[58] X. Wang, T. Luo, Q. Li, X. Cheng, K. Li, High performance aperiodic metal-dielectric multilayer stacks for solar energy thermal conversion, Sol. Energy Mater. Sol. Cells 191 (2019) 372–380, https://doi.org/10.1016/j.solmat.2018.12.006.
[59] H.D. Liu, T.R. Fu, M.H. Duan, Q. Wan, C. luo, Y.M. Chen, D.J. Fu, F. Ren, Q.Y. Li, X.D. Cheng, B. Yang, X.J. Hu, Structure and thermal stability of spectrally selective absorber based on AlCrON coating for solar-thermal conversion applications, Sol. Energy Mater. Sol. Cells 157 (2016) 108–116, https://doi.org/10.1016/j.solmat.2016.05.035.
[60] B. Chen, D. Yang, P.A. Charpentier, S. Nikumb, Optical and structural properties of pulsed laser deposited Ti:Al2O3 thin films, Sol. Energy Mater. Sol. Cells 92 (2008) 1025–1029, https://doi.org/10.1016/j.solmat.2008.03.004.
[61] D.M. Mattox, Handbook of Physical Vapor Deposition (PVD) Processing : Includes Index, 2010.
[62] R. Eason, Pulsed Laser Deposition of Thin Films : Applications-Led Growth of Functional Materials, Wiley-Interscience, Hoboken, N.J, 2010.
[63] T.K. Tsai, S.J. Hsueh, J.H. Lee, J.S. Fang, Optical properties and durability of Al2O3-NiP/Al solar absorbers prepared by electroless nickel composite plating, J. Electron. Mater. 41 (2012) 53–59, https://doi.org/10.1007/s11664-011-1746-2.
[64] R. Ghosh, H.K. Thota, R.U. Rani, Silicate spray-coated nickel-plated titanium alloy for space applications: corrosion resistance and thermo-optical properties, J. Mater. Eng. Perform. 30 (2021) 1378–1386, https://doi.org/10.1007/s11665-020-05347-y.
[65] N.N.A. Azli, N.F. Mohd Amin, S.T. Oluhende, S.N.A. Mohamad, N.A. Fadil, Electroless deposited black nickel-phosphorous solar absorber coatings on carbon steel: effect of plating bath pH, Mater. Today Proc. 39 (2021) 1071–1076, https://doi.org/10.1016/j.matpr.2020.06.087.
[66] G.O. Mallory, J.B. Hajdu, Electroless Plating : Fundamentals and Applications, American Electroplaters and Surface Finishers, New York, 2009.
[67] M.A.R. Khollari, M. Ghorbani, A. Afshar, Fabrication and characterization of TiO2 deposited black electroless Ni-P solar absorber, Appl. Surf. Sci. 496 (2019), 143632, https://doi.org/10.1016/J.APSUSC.2019.143632.
[68] M. Paunovic, M. Schlesinger, E. Society, Fundamentals of Electrochemical Deposition, John Wiley & Sons, Hoboken, NJ, 2006.
[69] E. Zäll, A. Nordenström, J. Mossegård, T. Wågberg, Electroplating of selective surfaces for concentrating solar collectors, in: Proc. EuroSun 2018, International Solar Energy Society, Freiburg, Germany, 2018, pp. 1–10, https://doi.org/10.18086/eurosun2018.10.09.
[70] S.K. Sharma, N.C. Mehra, Spectrally selective black nickel coating prepared by a conversion process, Thin Solid Films 213 (1992) 80–85, https://doi.org/10.1016/0040-6090(92)90478-T.
[71] J.D. Garrison, An electroplated nickel selective absorber, Sol. Energy Mater. 9 (1984) 483–492, https://doi.org/10.1016/0165-1633(84)90021-2.
[72] M. Köhl, K. Gindele, M. Mast, Selective nickel oxide solar absorber coatings electroplated with pulsed currents, Thin Solid Films 126 (1985) 11–16, https://doi.org/10.1016/0040-6090(85)90168-3.
[73] F. Jahan, B.E. Smith, Investigation of solar selective and microstructural properties of molybdenum black immersion coatings on cobalt substrates, J. Mater. Sci. 27 (1992) 625–636, https://doi.org/10.1007/BF00554027.
[74] S. John, S. Santhi, Electroplated cobalt-cadmium selective solar absorbers, Sol. Energy Mater. Sol. Cells 33 (1994) 505–516, https://doi.org/10.1016/0927-0248(94)90010-8.
[75] E. Wäckelgård, Characterization of black nickel solar absorber coatings electroplated in a nickel chlorine aqueous solution, Sol. Energy Mater. Sol. Cells 56 (1998) 35–44, https://doi.org/10.1016/S0927-0248(98)00113-5.
[76] M.K.A. Khan, Technical note Copper oxide coatings for use in a linear solar Fresnel reflecting concentrating collector, Renew. Energy 17 (1999) 603–608, https://doi.org/10.1016/S0960-1481(98)00023-8.
[77] K.D. Lee, Preparation and characterization of black cobalt solar selective coatings, J. Kor. Phys. Soc. 57 (2010) 111–119, https://doi.org/10.3938/jkps.57.111.
[78] M. Nashun, K. Kagimoto, N. Umeda Iwami, Simultaneous fabrication of a microcavity absorber-emitter on a Ni-W alloy film, Jpn. J. Appl. Phys. 56 (2017), https://doi.org/10.7567/JJAP.56.100310.
[79] R. Katırcı, A black electrodeposited copper–tin (Cu–Sn) alloy film for solar thermal absorbers, Trans. IMF. 96 (2018) 41–45, https://doi.org/10.1080/00202967.2018.1403084.
[80] S. Müller, F. Giovannetti, R. Reineke-Koch, O. Kastner, B. Hafner, Simulation study on the efficiency of thermochromic absorber coatings for solar thermal flat-plate collectors, Sol. Energy 188 (2019) 865–874, https://doi.org/10.1016/j.solener.2019.06.064.
[81] W. Zhou, Nanoimprint Lithography : an Enabling Process for Nanofabrication, Springer, Berlin, Heidelberg, 2016.
[82] H. Sai, Y. Kanamori, Spectrally selective thermal radiators and absorbers with periodic microstructured surface for high-temperature applications, Microscale Thermophys. Eng. 7 (2003) 101–115, https://doi.org/10.1080/10893950390203305.
[83] C.A. Mack, The new, new limits of optical lithography, in: R.S. Mackay (Ed.), Emerg. Lithogr. Technol. VIII, SPIE, 2004, pp. 1–8, https://doi.org/10.1117/12.546201.
[84] L.A. Weinstein, J. Loomis, B. Bhatia, D.M. Bierman, E.N. Wang, G. Chen, Concentrating solar power, Chem. Rev. 115 (2015) 12797–12838, https://doi.org/10.1021/acs.chemrev.5b00397.
[85] R. Kumar P, U. B, H.C. Barshilia, B. Basu, On the origin of spectrally selective high solar absorptance of TiB2-based tandem absorber with double layer antireflection coatings, Sol. Energy Mater. Sol. Cells 220 (2021), 110839, https://doi.org/10.1016/j.solmat.2020.110839.
[86] J.-Z. Lu, B.-H. Chen, L.-H. Jin, Z. Fang, G. Liu, X.-H. Gao, Thermal stability investigation of the SS/MO/Al2O3 spectrally selective solar absorber coatings, Surf. Eng. 35 (2019) 565–572, https://doi.org/10.1080/02670844.2018.1537083.
[87] X.-L. Qiu, X.-H. Gao, C.-Y. He, B.-H. Chen, G. Liu, Structure{,} optical simulation and thermal stability of the HfB2-based high-temperature solar selective absorbing coatings, RSC Adv. 9 (2019) 29726–29733, https://doi.org/10.1039/C9RA05014K.
[88] A. Dan, J. Jyothi, K. Chattopadhyay, H.C. Barshilia, B. Basu, Spectrally selective absorber coating of WAlN/WAlON/Al2O3 for solar thermal applications, Sol. Energy Mater. Sol. Cells 157 (2016) 716–726, https://doi.org/10.1016/j.solmat.2016.07.018.
[89] E.B. Rubin, Y. Chen, R. Chen, Optical properties and thermal stability of Cu spinel oxide nanoparticle solar absorber coatings, Sol. Energy Mater. Sol. Cells 195 (2019) 81–88, https://doi.org/10.1016/J.SOLMAT.2019.02.032.

[90] D.E. Karas, J. Byun, J. Moon, C. Jose, Copper-oxide spinel absorber coatings for high-temperature concentrated solar power systems, Sol. Energy Mater. Sol. Cells 182 (2018) 321–330, https://doi.org/10.1016/J.SOLMAT.2018.03.025.
[91] H. Tabor, Receiver for Solar Energy Collectors, US2917817A, 1959.
[92] C.E. Kennedy, Review of Mid- to High- Temperature Solar Selective Absorber Materials, 2002. Golden, Colorado, USA.
[93] J. Moon, D. Lu, B. VanSaders, T.K. Kim, S.D. Kong, S. Jin, R. Chen, Z. Liu, High performance multi-scaled nanostructured spectrally selective coating for concentrating solar power, Nano Energy 8 (2014) 238–246, https://doi.org/10.1016/j.nanoen.2014.06.016.
[94] N.P. Sergeant, O. Pincon, M. Agrawal, P. Peumans, Design of wide-angle solar-selective absorbers using aperiodic metal-dielectric stacks, Opt Express 17 (2009) 22800, https://doi.org/10.1364/oe.17.022800.
[95] Photonic Crystals - Latest Research and News | Nature, (n.d.). https://www.nature.com/subjects/photonic-crystals (accessed January 15, 2021).
[96] F. Cao, K. McEnaney, G. Chen, Z. Ren, A review of cermet-based spectrally selective solar absorbers, Energy Environ. Sci. 7 (2014) 1615–1627, https://doi.org/10.1039/c3ee43825b.
[97] F. Cao, L. Tang, Y. Li, A.P. Litvinchuk, J. Bao, Z. Ren, A high-temperature stable spectrally-selective solar absorber based on cermet of titanium nitride in SiO2 deposited on lanthanum aluminate, Sol. Energy Mater. Sol. Cells 160 (2017) 12–17, https://doi.org/10.1016/j.solmat.2016.10.012.
[98] A. Boubault, C.K. Ho, A. Hall, T.N. Lambert, A. Ambrosini, Durability of solar absorber coatings and their cost-effectiveness, Sol. Energy Mater. Sol. Cells 166 (2017) 176–184, https://doi.org/10.1016/j.solmat.2017.03.010.
[99] L. Noč, E. Šest, G. Kapun, F. Ruiz-Zepeda, Y. Binyamin, F. Merzel, I. Jerman, High-solar-absorptance CSP coating characterization and reliability testing with isothermal and cyclic loads for service-life prediction, Energy Environ. Sci. (2019) 1679–1694, https://doi.org/10.1039/C8EE03536A.
[100] K. Zhang, L. Hao, M. Du, J. Mi, J.-N. Wang, J. Meng, A review on thermal stability and high temperature induced ageing mechanisms of solar absorber coatings, Renew. Sustain. Energy Rev. 67 (2017) 1282–1299, https://doi.org/10.1016/j.rser.2016.09.083.
[101] E. Zäll, A. Nordenström, J. Mossegård, T. Wågberg, Electroplating of selective surfaces for concentrating solar collectors, in: Proc. EuroSun 2018, International Solar Energy Society, Freiburg, Germany, 2018, pp. 1–10, https://doi.org/10.18086/eurosun2018.10.09.
[102] B.H. Chandra, Solar Selective Coating Having High Thermal Stability and A Process for the Preparation Thereof, US 9803891 B2, 2017.
[103] A. Boubault, C.K. Ho, A. Hall, T.N. Lambert, A. Ambrosini, Levelized cost of energy (LCOE) metric to characterize solar absorber coatings for the CSP industry, Renew. Energy 85 (2016) 472–483, https://doi.org/10.1016/j.renene.2015.06.059.
[104] C.K. Ho, A.R. Mahoney, A. Ambrosini, M. Bencomo, A. Hall, T.N. Lambert, Characterization of Pyromark 2500 paint for high-temperature solar receivers, J. Sol. Energy Eng. 136 (2013), https://doi.org/10.1115/1.4024031.
[105] N. Martínez, A. Rico, C.J. Múnez, C. Prieto, P. Poza, Improving durability of silicone-based paint coatings used in solar power plants by controlling consolidation procedures, Sol. Energy 199 (2020) 585–595, https://doi.org/10.1016/j.solener.2020.02.049.
[106] R. Reoyo-Prats, A. Carling Plaza, O. Faugeroux, B. Claudet, A. Soum-Glaude, C. Hildebrandt, Y. Binyamin, A. Agüero, T. Meißner, Accelerated aging of absorber coatings for CSP receivers under real high solar flux – evolution of their optical properties, Sol. Energy Mater. Sol. Cells 193 (2019) 92–100, https://doi.org/10.1016/j.solmat.2018.12.030.
[107] C. Xu, E. Lee, X. Wang, J. Liu, High-efficiency, high-temperature, air-stable Cu, Mn and Fe oxides nanoparticles-pigmented silicone solar selective coatings via hot spray-coating method, in: OSA Adv. Photonics Congr. 2019 (IPR, Networks, NOMA, SPPCom, PVLED), Optical Society of America, 2019, https://doi.org/10.1364/PVLED.2019.PW3C.6. PW3C.6.
[108] X. Wang, X. Yu, S. Fu, E. Lee, K. Kekalo, J. Liu, Design and optimization of nanoparticle-pigmented solar selective absorber coatings for high-temperature concentrating solar thermal systems, J. Appl. Phys. 123 (2018), 33104, https://doi.org/10.1063/1.5009252.
[109] X. Wang, E. Lee, C. Xu, J. Liu, High-efficiency, air-stable manganese–iron oxide nanoparticle-pigmented solar selective absorber coatings toward concentrating solar power systems operating at 750 °C, Mater. Today Energy 19 (2021), 100609, https://doi.org/10.1016/j.mtener.2020.100609.
[110] M. Mehos, C. Turchi, J. Vidal, M. Wagner, Z. Ma, C. Ho, W. Kolb, C. Andraka, M. Mehos, C. Turchi, J. Vidal, M. Wagner, Z. Ma, C. Ho, W. Kolb, C. Andraka, A. Kruizenga, NREL, Concentrating Solar Power Gen3 Demonstration Roadmap, 2017, https://doi.org/10.2172/1338899.
[111] A.A. Shah, M.C. Gupta, Spectral selective surfaces for concentrated solar power receivers by laser sintering of tungsten micro and nano particles, Sol. Energy Mater. Sol. Cells 117 (2013) 489–493, https://doi.org/10.1016/j.solmat.2013.07.013.
[112] J. Aranovich, B.O. Seraphin, Solar Energy Conversion Solid-State Physics Aspects, Springer Berlin, Berlin, 2014.
[113] K. Hans, S. Latha, P. Bera, H.C. Barshilia, Hafnium carbide based solar absorber coatings with high spectral selectivity, Sol. Energy Mater. Sol. Cells 185 (2018) 1–7, https://doi.org/10.1016/J.SOLMAT.2018.05.005.
[114] X.-H. Gao, X.-L. Qiu, X.-T. Li, W. Theiss, B.-H. Chen, H.-X. Guo, T.-H. Zhou, G. Liu, Structure, thermal stability and optical simulation of ZrB2 based spectrally selective solar absorber coatings, Sol. Energy Mater. Sol. Cells 193 (2019) 178–183, https://doi.org/10.1016/J.SOLMAT.2018.12.040.
[115] A. Roos, M. Georgson, Tin-oxide-coated anodized aluminium selective absorber surfaces II. Aging and durability, Sol. Energy Mater. 22 (1991) 29–41, https://doi.org/10.1016/0165-1633(91)90004-5.
[116] K. Chidambaram, L.K. Malhotra, K.L. Chopra, Spray-pyrolysed cobalt black as a high temperature selective absorber, Thin Solid Films 87 (1982) 365–371, https://doi.org/10.1016/0040-6090(82)90289-9.
[117] D. Sciti, L. Silvestroni, J.-L. Sans, L. Mercatelli, M. Meucci, E. Sani, Tantalum diboride-based ceramics for bulk solar absorbers, Sol. Energy Mater. Sol. Cells 130 (2014) 208–216, https://doi.org/10.1016/J.SOLMAT.2014.07.012.
[118] R. Akoba, G.G. Welegergs, M. Luleka, J. Sackey, N. Nauman, B.M. Mothudi, Z. Y. Nuru, M. Maaza, Effect of etchant concentration on the optical properties and surface topography of MoO3 selective solar absorber thin films, MRS Adv 5 (2020) 1133–1143, https://doi.org/10.1557/adv.2020.194.
[119] D.M. Mattox, G.J. Kominiak, Deposition of semiconductor films with high solar absorptivity, J. Vac. Sci. Technol. 12 (1975) 182–185, https://doi.org/10.1116/1.568750.
[120] D.E. Ackley, J. Tauc, Silicon films as selective absorbers for solar energy conversion, Appl. Opt. 16 (1977) 2806, https://doi.org/10.1364/AO.16.002806.
[121] P.J. Martin, R.P. Netterfield, W.G. Sainty, Spectrally selective PbS films produced by ion beam sputtering, Thin Solid Films 87 (1982) 203–206, https://doi.org/10.1016/0040-6090(82)90357-1.
[122] A. Slonopas, N. Alijabbari, C. Saltonstall, T. Globus, P. Norris, Chemically deposited nanocrystalline lead sulfide thin films with tunable properties for use in photovoltaics, Electrochim. Acta 151 (2015) 140–149, https://doi.org/10.1016/J.ELECTACTA.2014.11.021.
[123] S.B. Gadgil, R. Thangaraj, O.P. Agnihotri, Optical and solar selective properties of chemically sprayed copper sulphide films, J. Phys. D Appl. Phys. 20 (1987) 112–115, https://doi.org/10.1088/0022-3727/20/1/017.
[124] Z. Chen, T. Boström, Electrophoretically deposited carbon nanotube spectrally selective solar absorbers, Sol. Energy Mater. Sol. Cells 144 (2016) 678–683, https://doi.org/10.1016/j.solmat.2015.10.016.
[125] R. Subasri, K.R.C. Soma Raju, D.S. Reddy, N.Y. Hebalkar, G. Padmanabham, Sol–gel derived solar selective coatings on SS 321 substrates for solar thermal applications, Thin Solid Films 598 (2016) 46–53, https://doi.org/10.1016/j.tsf.2015.12.002.
[126] D. Yang, X. Zhao, Y. Liu, J. Li, H. Liu, X. Hu, Z. Li, J. Zhang, J. Guo, Y. Chen, B. Yang, Enhanced thermal stability of solar selective absorber based on nano-multilayered AlCrSiO films, Sol. Energy Mater. Sol. Cells 207 (2020), 110331, https://doi.org/10.1016/j.solmat.2019.110331.
[127] X. Wang, K. Li, X. Cheng, Resistant transition-metal-nitrides based coatings for solar energy conversion, J. Eur. Ceram. Soc. (2021), https://doi.org/10.1016/j.jeurceramsoc.2021.02.001.
[128] T.C. Rojas, A. Caro, R. Escobar-Galindo, J.C. Sánchez-López, High-temperature solar-selective coatings based on Cr(Al)N. Part 2: design, spectral properties and thermal stability of multilayer stacks, Sol. Energy Mater. Sol. Cells 218 (2020), 110812, https://doi.org/10.1016/j.solmat.2020.110812.
[129] H.-X. Guo, D.-M. Yu, C.-Y. He, X.-L. Qiu, S.-S. Zhao, G. Liu, X.-H. Gao, Double-layer solar absorber coating based on high entropy ceramic AlCrMoTaTiN: structure, optical properties and failure mechanism, Surface. Interfac. (2021), 101062, https://doi.org/10.1016/j.surfin.2021.101062.
[130] A. Al-Rjoub, L. Rebouta, N.F. Cunha, F. Fernandes, N.P. Barradas, E. Alves, W/AlSiTiNx/SiAlTiOyNx/SiAlOx multilayered solar thermal selective absorber coating, Sol. Energy 207 (2020) 192–198, https://doi.org/10.1016/j.solener.2020.06.094.
[131] A. Dan, K. Chattopadhyay, H.C. Barshilia, B. Basu, Colored selective absorber coating with excellent durability, Thin Solid Films 620 (2016) 17–22, https://doi.org/10.1016/j.tsf.2016.08.070.
[132] S.-S. Zhao, X.-H. Gao, X.-L. Qiu, D.-M. Yu, G.-K. Tian, A novel TiC-TiN based spectrally selective absorbing coating: structure, optical properties and thermal stability, Infrared Phys. Technol. 110 (2020), 103471, https://doi.org/10.1016/j.infrared.2020.103471.
[133] M. Bello, S. Subramani, M.M. Bin Mohd Rashid, The impact of Fe3O4 on the performance of ultrathin Ti/AlN/Ti tandem coating on stainless-steel for solar selective absorber application, Results Phys. 19 (2020), 103582, https://doi.org/10.1016/j.rinp.2020.103582.
[134] C.-Y. He, X.-L. Qiu, D.-M. Yu, S.-S. Zhao, H.-X. Guo, G. Liu, X.-H. Gao, Greatly enhanced solar absorption via high entropy ceramic AlCrTaTiZrN based solar selective absorber coatings, J. Mater. 7 (2021) 460–469, https://doi.org/10.1016/j.jmat.2020.11.010.
[135] C.-Y. He, X.-H. Gao, D.-M. Yu, X.-L. Qiu, H.-X. Guo, G. Liu, Scalable and highly efficient high temperature solar absorber coatings based on high entropy alloy nitride AlCrTaTiZrN with different antireflection layers, J. Mater. Chem. (2021), https://doi.org/10.1039/D0TA09988K.
[136] C.-Y. He, X.-H. Gao, X.-L. Qiu, D.-M. Yu, H.-X. Guo, G. Liu, Scalable and ultrathin high-temperature solar selective absorbing coatings based on the high-entropy nanoceramic AlCrWTaNbTiN with high photothermal conversion efficiency, Sol. RRL. n/a (n.d.). doihttps://doi.org/10.1002/solr.202000790.
[137] A. Al-Rjoub, L. Rebouta, P. Costa, N.P. Barradas, E. Alves, P.J. Ferreira, K. Abderrafi, A. Matilainen, K. Pischow, A design of selective solar absorber for high temperature applications, Sol. Energy 172 (2018) 177–183, https://doi.org/10.1016/J.SOLENER.2018.04.052.
[138] A. Soum-Glaude, A. Le Gal, M. Bichotte, C. Escape, L. Dubost, Optical characterization of TiAlNx/TiAlNy/Al2O3 tandem solar selective absorber coatings, Sol. Energy Mater. Sol. Cells 170 (2017) 254–262, https://doi.org/10.1016/J.SOLMAT.2017.06.007.

[139] P. Kondaiah, K. Niranjan, S. John, H.C. Barshilia, Tantalum carbide based spectrally selective coatings for solar thermal absorber applications, Sol. Energy Mater. Sol. Cells 198 (2019) 26–34, https://doi.org/10.1016/J.SOLMAT.2019.04.016.
[140] X.-L. Qiu, X.-H. Gao, T.-H. Zhou, B.-H. Chen, J.-Z. Lu, H.-X. Guo, X.-T. Li, G. Liu, Structure, thermal stability and chromaticity investigation of TiB2 based high temperature solar selective absorbing coatings, Sol. Energy 181 (2019) 88–94, https://doi.org/10.1016/J.SOLENER.2019.01.068.
[141] X. Wang, T. Luo, Q. Li, X. Cheng, K. Li, High performance aperiodic metal-dielectric multilayer stacks for solar energy thermal conversion, Sol. Energy Mater. Sol. Cells 191 (2019) 372–380, https://doi.org/10.1016/J.SOLMAT.2018.12.006.
[142] J. Jyothi, H. Chaliyawala, G. Srinivas, H.S. Nagaraja, H.C. Barshilia, Design and fabrication of spectrally selective TiAlC/TiAlCN/TiAlSiCN/TiAlSiCO/TiAlSiO tandem absorber for high-temperature solar thermal power applications, Sol. Energy Mater. Sol. Cells 140 (2015) 209–216, https://doi.org/10.1016/J.SOLMAT.2015.04.018.
[143] H. Wang, H. Alshehri, H. Su, L. Wang, Design, fabrication and optical characterizations of large-area lithography-free ultrathin multilayer selective solar coatings with excellent thermal stability in air, Sol. Energy Mater. Sol. Cells 174 (2018) 445–452, https://doi.org/10.1016/J.SOLMAT.2017.09.025.
[144] N. Selvakumar, H.C. Barshilia, K.S. Rajam, A. Biswas, Structure, optical properties and thermal stability of pulsed sputter deposited high temperature HfOx/Mo/HfO2 solar selective absorbers, Sol. Energy Mater. Sol. Cells 94 (2010) 1412–1420, https://doi.org/10.1016/J.SOLMAT.2010.04.073.
[145] L. Hao, S. Wang, L. Jiang, X. Liu, H. Li, Z. Li, Preparation and thermal stability on non-vacuum high temperature solar selective absorbing coatings, Chin. Sci. Bull. 54 (2009) 1451–1454, https://doi.org/10.1007/s11434-009-0159-6.
[146] M. Bilokur, A.R. Gentle, M.D. Arnold, M.B. Cortie, G.B. Smith, High temperature optically stable spectrally-selective Ti1-xAlxN-based multilayer coating for concentrated solar thermal applications, Sol. Energy Mater. Sol. Cells 200 (2019), 109964, https://doi.org/10.1016/J.SOLMAT.2019.109964.
[147] M.S. Prasad, B. Mallikarjun, M. Ramakrishna, J. Joarder, B. Sobha, S. Sakthivel, Zirconia nanoparticles embedded spinel selective absorber coating for high performance in open atmospheric condition, Sol. Energy Mater. Sol. Cells 174 (2018) 423–432, https://doi.org/10.1016/J.SOLMAT.2017.09.032.
[148] H.D. Liu, B. Yang, M.R. Mao, Y. Liu, Y.M. Chen, Y. Cai, D.J. Fu, F. Ren, Q. Wan, X. J. Hu, Enhanced thermal stability of solar selective absorber based on nano-multilayered TiAlON films deposited by cathodic arc evaporation, Appl. Surf. Sci. 501 (2020), 144025, https://doi.org/10.1016/J.APSUSC.2019.144025.
[149] Y. Yang, T. Wang, T. Yao, G. Li, Y. Sun, X. Cao, L. Ma, S. Peng, Preparation of a novel TiN/TiNxOy/SiO2 composite ceramic films on aluminum substrate as a solar selective absorber by magnetron sputtering, J. Alloys Compd. 815 (2020), 152209, https://doi.org/10.1016/J.JALLCOM.2019.152209.
[150] X.-H. Gao, X.-L. Qiu, Y.-Q. Shen, C.-Y. He, G. Liu, A novel TiC–ZrB2/ZrB2/Al2O3 multilayer high temperature solar selective absorbing coating: microstructure, optical properties and failure mechanism, Sol. Energy Mater. Sol. Cells 203 (2019), 110187, https://doi.org/10.1016/J.SOLMAT.2019.110187.
[151] K. Niranjan, P. Kondaiah, G. Srinivas, H.C. Barshilia, Optimization of W/WAlSiN/SiON/SiO2 tandem absorber consisting of double layer anti-reflection coating with broadband absorption in the solar spectrum region, Appl. Surf. Sci. 496 (2019), 143651, https://doi.org/10.1016/J.APSUSC.2019.143651.
[152] F. Chen, S.-W. Wang, X. Liu, R. Ji, L. Yu, X. Chen, W. Lu, High performance colored selective absorbers for architecturally integrated solar applications, J. Mater. Chem. A. 3 (2015) 7353–7360, https://doi.org/10.1039/C5TA00694E.
[153] S.R. Atchuta, S. Sakthivel, H.C. Barshilia, Nickel doped cobaltite spinel as a solar selective absorber coating for efficient photothermal conversion with a low thermal radiative loss at high operating temperatures, Sol. Energy Mater. Sol. Cells 200 (2019), 109917, https://doi.org/10.1016/J.SOLMAT.2019.109917.
[154] X.-H. Gao, Z.-M. Guo, Q.-F. Geng, P.-J. Ma, A.-Q. Wang, G. Liu, Structure{,} optical properties and thermal stability of SS/TiC–ZrC/Al2O3 spectrally selective solar absorber, RSC Adv. 6 (2016) 63867–63873, https://doi.org/10.1039/C6RA11602G.
[155] N. Selvakumar, A. Biswas, D.V.S. Rao, S.B. Krupanidhi, H.C. Barshilia, Role of component layers in designing carbon nanotubes-based tandem absorber on metal substrates for solar thermal applications, Sol. Energy Mater. Sol. Cells 155 (2016) 397–404, https://doi.org/10.1016/j.solmat.2016.06.051.
[156] X. Wang, H. He, J. Gao, H. Hu, S. Tang, X. Li, X. Li, H. Cao, Effects of nanoparticle structural features on the light-matter interactions in nanocermet layers and cermet-based solar absorbers, J. Mater. (2021), https://doi.org/10.1016/j.jmat.2021.01.011.
[157] T.S. Sathiaraj, R. Thangaraj, H. Al Sharbaty, M. Bhatnagar, O.P. Agnihotri, Ni-Al2O3 selective cermet coatings for photothermal conversion up to 500°C, Thin Solid Films 190 (1990) 241–254, https://doi.org/10.1016/0040-6090(89)90914-0.
[158] A. Antonaia, A. Castaldo, M.L. Addonizio, S. Esposito, Stability of W-Al2O3 cermet based solar coating for receiver tube operating at high temperature, Sol. Energy Mater. Sol. Cells 94 (2010) 1604–1611, https://doi.org/10.1016/J.SOLMAT.2010.04.080.
[159] H.C. Barshilia, P. Kumar, K.S. Rajam, A. Biswas, Structure and optical properties of Ag–Al2O3 nanocermet solar selective coatings prepared using unbalanced magnetron sputtering, Sol. Energy Mater. Sol. Cells 95 (2011) 1707–1715, https://doi.org/10.1016/J.SOLMAT.2011.01.034.
[160] F. Cao, D. Kraemer, T. Sun, Y. Lan, G. Chen, Z. Ren, Enhanced thermal stability of W-Ni-Al 2 O 3 cermet-based spectrally selective solar absorbers with tungsten infrared reflectors, Adv. Energy Mater. 5 (2015), 1401042, https://doi.org/10.1002/aenm.201401042.
[161] Q.-C. Zhang, Metal-{AlN} cermet solar selective coatings deposited by direct current magnetron sputtering technology, J. Phys. D Appl. Phys. 31 (1998) 355–362, https://doi.org/10.1088/0022-3727/31/4/003.
[162] R.B. Pettit, R.R. Sowell, I.J. Hall, Black chrome solar selective coatings optimized for high temperature applications, Sol. Energy Mater. 7 (1982) 153–170, https://doi.org/10.1016/0165-1633(82)90081-8.
[163] L. Zheng, F. Zhou, Z. Zhou, X. Song, G. Dong, M. Wang, X. Diao, Angular solar absorptance and thermal stability of Mo-SiO2 double cermet solar selective absorber coating, Sol. Energy 115 (2015), https://doi.org/10.1016/j.solener.2015.02.013.
[164] D. Ding, K. Liu, Q. Fan, B. Dong, Y. Zhang, Y. Yin, C. Gao, S. Ding, Nickel nanoparticles individually encapsulated in densified ceramic shells for thermally stable solar energy absorption, J. Mater. Chem. A. 7 (2019) 3039–3045, https://doi.org/10.1039/C8TA10690H.
[165] F. Cao, D. Kraemer, L. Tang, Y. Li, A.P. Litvinchuk, J. Bao, G. Chen, Z. Ren, A high-performance spectrally-selective solar absorber based on a yttria-stabilized zirconia cermet with high-temperature stability, Energy Environ. Sci. 8 (2015) 3040–3048, https://doi.org/10.1039/C5EE02066B.
[166] Y. Ning, J. Wang, C. Ou, C. Sun, Z. Hao, B. Xiong, L. Wang, Y. Han, H. Li, Y. Luo, NiCr–MgF2 spectrally selective solar absorber with ultra-high solar absorptance and low thermal emittance, Sol. Energy Mater. Sol. Cells (2019), 110219, https://doi.org/10.1016/J.SOLMAT.2019.110219.
[167] L. Noč, F. Ruiz-Zepeda, F. Merzel, I. Jerman, High-temperature "ion baseball" for enhancing concentrated solar power efficiency, Sol. Energy Mater. Sol. Cells 200 (2019) 109974, https://doi.org/10.1016/J.SOLMAT.2019.109974.
[168] D.E. Karas, J. Byun, J. Moon, C. Jose, Copper-oxide spinel absorber coatings for high-temperature concentrated solar power systems, Sol. Energy Mater. Sol. Cells 182 (2018) 321–330, https://doi.org/10.1016/j.solmat.2018.03.025.
[169] T. Abendroth, H. Althues, G. Mäder, P. Härtel, S. Kaskel, E. Beyer, Selective absorption of Carbon Nanotube thin films for solar energy applications, Sol. Energy Mater. Sol. Cells 143 (2015) 553–556, https://doi.org/10.1016/j.solmat.2015.07.044.
[170] H. El Aakib, N. Rochdi, J.F. Pierson, A. Outzourhit, Reactively sputtered cobalt oxide coatings for solar selective absorber applications, Mater, Today Proc 39 (2021) 1157–1162, https://doi.org/10.1016/j.matpr.2020.07.562.
[171] H. Wang, V. Prasad Sivan, A. Mitchell, G. Rosengarten, P. Phelan, L. Wang, Highly efficient selective metamaterial absorber for high-temperature solar thermal energy harvesting, Sol. Energy Mater. Sol. Cells 137 (2015) 235–242, https://doi.org/10.1016/J.SOLMAT.2015.02.019.
[172] P. Li, B. Liu, Y. Ni, K.K. Liew, J. Sze, S. Chen, S. Shen, Large-scale nanophotonic solar selective absorbers for high-efficiency solar thermal energy conversion, Adv. Mater. 27 (2015) 4585–4591, https://doi.org/10.1002/adma.201501686.
[173] M. Bichotte, T. Kämpfe, W. Iff, F. Celle, S. Reynaud, D. Jamon, T. Pouit, A. Soum-Glaude, A. Keilany, L. Dubost, Y. Jourlin, Diffractive gratings to improve TiAlN based spectrally selective solar absorbers, AIP Conf. Proc. 2033 (2018) 40007, https://doi.org/10.1063/1.5067043.
[174] M. He, Y. Wang, H. Wang, R. Chen, A one-step sol-gel route derived Ag-CuO film as a novel solar selective absorber, Sol. Energy Mater. Sol. Cells 144 (2016) 264–272, https://doi.org/10.1016/j.solmat.2015.09.025.
[175] X.-H. Gao, Z.-M. Guo, Q.-F. Geng, P.-J. Ma, G. Liu, Enhanced absorptance of surface-textured tungsten thin film for solar absorber, Surf. Eng. 32 (2016) 840–845, https://doi.org/10.1080/02670844.2016.1187466.
[176] X.-H. Gao, Z.-M. Guo, Q.-F. Geng, P.-J. Ma, G. Liu, Microstructure and optical properties of SS/Mo/Al2O3 spectrally selective solar absorber coating, J. Mater. Eng. Perform. 26 (2017) 161–167, https://doi.org/10.1007/s11665-016-2445-1.
[177] I. Celanovic, N. Jovanovic, J. Kassakian, Two-dimensional tungsten photonic crystals as selective thermal emitters, Appl. Phys. Lett. 92 (2008), 193101, https://doi.org/10.1063/1.2927484.
[178] V. Stelmakh, V. Rinnerbauer, R.D. Geil, P.R. Aimone, J.J. Senkevich, J. D. Joannopoulos, M. Soljačić, I. Celanovic, High-temperature tantalum tungsten alloy photonic crystals: stability, optical properties, and fabrication, Appl. Phys. Lett. 103 (2013), https://doi.org/10.1063/1.4821586.
[179] V. Rinnerbauer, E. Lausecker, F. Schäffler, P. Reininger, G. Strasser, R.D. Geil, J. D. Joannopoulos, M. Soljačić, I. Celanovic, Nanoimprinted superlattice metallic photonic crystal as ultraselective solar absorber, Optica 2 (2015) 743–746, https://doi.org/10.1364/OPTICA.2.000743.
[180] J.B. Chou, Y.X. Yeng, Y.E. Lee, A. Lenert, V. Rinnerbauer, I. Celanovic, M. Soljačić, N.X. Fang, E.N. Wang, S.-G. Kim, Enabling ideal selective solar absorption with 2D metallic dielectric photonic crystals, Adv. Mater. 26 (2014) 8041–8045, https://doi.org/10.1002/adma.201403302.
[181] R. Zhang, J. Cohen, S. Fan, P.V. Braun, Electrodeposited high strength{,} thermally stable spectrally selective rhenium nickel inverse opals, Nanoscale 9 (2017) 11187–11194, https://doi.org/10.1039/C7NR03567E.
[182] K.A. Arpin, M.D. Losego, A.N. Cloud, H. Ning, J. Mallek, N.P. Sergeant, L. Zhu, Z. Yu, B. Kalanyan, G.N. Parsons, G.S. Girolami, J.R. Abelson, S. Fan, P.V. Braun, Three-dimensional self-assembled photonic crystals with high temperature stability for thermal emission modification, Nat. Commun. 4 (2013) 2630, https://doi.org/10.1038/ncomms3630.
[183] W. Lipiński, E. Abbasi-Shavazi, J. Chen, J. Coventry, M. Hangi, S. Iyer, A. Kumar, L. Li, S. Li, J. Pye, J.F. Torres, B. Wang, Y. Wang, V.M. Wheeler, Progress in heat transfer research for high-temperature solar thermal applications, Appl. Therm. Eng. 184 (2021), 116137, https://doi.org/10.1016/j.applthermaleng.2020.116137.